Soomro *et al. Bioresources and Bioprocessing* (2026) 13:80
https://doi.org/10.1186/s40643-026-01067-8

Bioresources
and Bioprocessing

REVIEW Open Access

Biochar from food processing wastes: a multi-criteria roadmap for circular energy and environmental applications

Ahsanullah Soomro[1,2*], Anıl Tevfik Koçer[1,3] and Didem Balkanlı[1]

Abstract This review develops a region-specific Multi-Criteria Decision Analysis (MCDA)-based screening framework for evaluating food-processing residues for biochar applications, offering a transparent and replicable decision-support tool for policymakers and bioeconomy stakeholders in Turkey and beyond. Using Turkey as a region-specific case context, ten underutilized residues—boza fermentation residue, tarhana fines, rosehip seed cake, mulberry syrup press-cake, carob syrup pulp residue, pumpkin seed oil cake, saffron floral by-products, fig-jam seed fraction, lupin brining sediment, and date syrup filter cake—were compiled from the literature and characterized in terms of moisture, ash, organic fractions, higher heating value, and macro-mineral composition. Drawing on thermochemical fundamentals, the review synthesizes how these traits influence biochar properties relevant to fuel use, soil amendment, pollutant adsorption, anaerobic digestion (AD) enhancement, and composite materials, and qualitatively links residue groups to suitable conversion windows such as hydrothermal carbonization and low- or high-severity slow pyrolysis. To convert this information into a transparent screening tool, all indicators were normalized via min–max transformation and aggregated into four mechanistic proxies capturing fuel quality, nutrient release, an adsorption-oriented screening proxy, and AD compatibility. A Simple Additive Weighting (SAW) method was then used to calculate 0–1 suitability scores and 0–100 indices for five application domains: fuel, soil amendment, adsorption/remediation, AD enhancement, and composite/material use. Under the selected criteria and weighting assumptions, rosehip seed cake, pumpkin seed oil cake, carob syrup pulp residue, and fig-jam seed fraction emerged as comparatively high-priority feedstocks, whereas saffron floral by-products and lupin brining sediment showed consistently low relative suitability. By linking feedstock chemistry to application-oriented screening scores, the framework supports rapid comparison of residue-to-application pathways while acknowledging that rankings may evolve as additional performance data, logistical constraints, or alternative weighting scenarios are incorporated.

Keywords Biochar, Pyrolysis, Food-processing residues, Multi-criteria decision analysis (MCDA), Circular bioeconomy

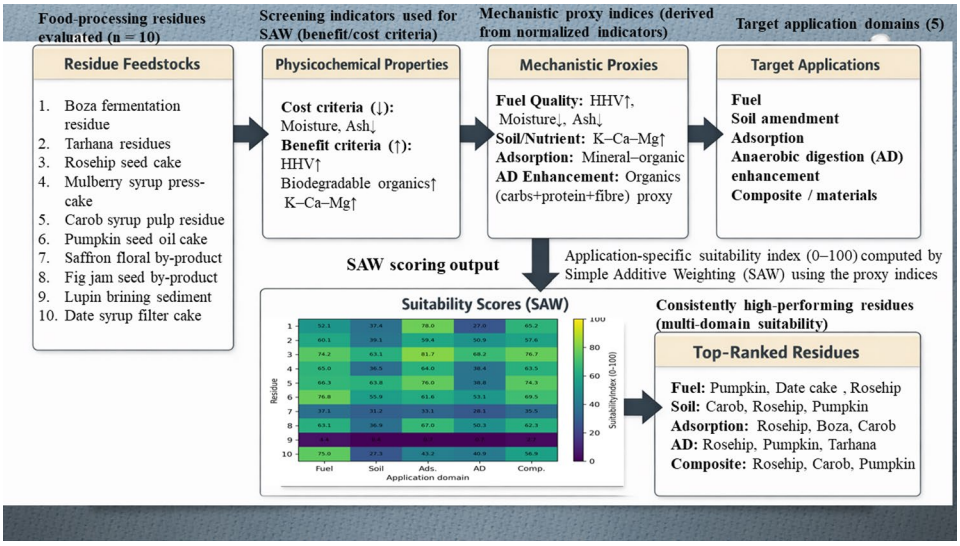
*Correspondence:
Ahsanullah Soomro
ahsanullah.soomro@yildiz.edu.tr

Full list of author information is available at the end of the article

© The Author(s) 2026. **Open Access** This article is licensed under a Creative Commons Attribution 4.0 International License, which permits use, sharing, adaptation, distribution and reproduction in any medium or format, as long as you give appropriate credit to the original author(s) and the source, provide a link to the Creative Commons licence, and indicate if changes were made. The images or other third party material in this article are included in the article's Creative Commons licence, unless indicated otherwise in a credit line to the material. If material is not included in the article's Creative Commons licence and your intended use is not permitted by statutory regulation or exceeds the permitted use, you will need to obtain permission directly from the copyright holder. To view a copy of this licence, visit http://creativecommons.org/licenses/by/4.0/.

Springer

Graphical abstract



Introduction

The generation of food-processing and biomass residues has become a pressing global issue, particularly in the context of expanding agri-food systems and unsustainable waste practices (Paritosh et al. 2017). In parallel, food-processing industries generate substantial quantities of compositionally distinct by-products and residue streams that often remain underutilized despite their considerable valorization potential (Khalid et al. 2025). A significant proportion of these residues originates from food-processing operations, where solid by-products are still commonly disposed of through open burning, landfilling, or unregulated dumping, resulting in the loss of valuable carbon and nutrients as well as increased environmental burdens (Siddiqua et al. 2022). These conventional disposal methods not only result in the release of greenhouse gases (GHGs) and short-lived climate pollutants, but also contribute to soil and water contamination while neglecting the recovery of valuable nutrients and carbon (Pierrehumbert 2014; Sharma et al. 2019; Singh et al. 2025).

In response to these challenges, the concept of a circular economy has gained traction, emphasizing the valorization of organic residues as secondary resources. Among the emerging strategies, biochar production through thermochemical conversion of biomass under oxygen-limited conditions has attracted significant global attention (Do and Nguyen 2024). Biochar offers a unique platform for resource recovery by stabilizing carbon, improving soil health, enhancing crop productivity, supporting renewable energy systems, and enabling pollutant remediation (Agegnehu et al. 2017; Liu et al. 2015). A recent global assessment indicated that biochar, when sustainably produced, could mitigate up to 6.2 ± 0.2% of anthropogenic GHG emissions over a 100-year horizon, with more than 10% reduction potential in several countries (Lefebvre et al. 2023). Global modelling indicates that biochar systems could remove between 2.6 and 10.3 Gt CO_2-equivalent per year, depending on deployment scale and feedstock use (Weng and Cowie 2025). Meta-analyses further highlight its multifunctionality, demonstrating benefits across agriculture, environmental engineering, and material science domains (Mohan et al. 2014; Sivaranjanee et al. 2024).

Although global interest in residue valorization is increasing, the suitability of food-industry residues for biochar production remains highly context-dependent and therefore requires region-specific assessment. In this review, Turkey is used as a case-study context because its agri-food sector includes several culturally embedded processing chains that generate underutilized residues such as boza, tarhana, rosehip oil, carob syrup, mulberry molasses, and pumpkin-seed oil by-products. The ten residues were selected as food-processing-specific and compositionally diverse side-streams with sufficient literature-reported physicochemical data for comparative biochar screening. Although precise national generation volumes are not uniformly available for all residues, each is linked to established processing activities and recurring regional production. The aim was not to represent all biomass resources in the country; accordingly, several larger-volume and already well-studied residues were not prioritized in this review. National resource-flow assessments suggest that fruit-pruning residues alone could yield approximately 175,000 tonnes of biochar annually through slow pyrolysis, highlighting the significant

untapped potential for biochar deployment in the country (Dursun 2024). Despite this opportunity, there is a lack of comprehensive studies addressing the physicochemical characteristics, thermochemical conversion compatibility, and biochar application pathways for many of these niche residues.

In parallel with food-industry valorization, recent research in Turkey has increasingly focused on the conversion of algal biomass into biofuels. Microalgae are either collected from coastal environments (Koçer and Özçimen 2018, 2024; Özçimen et al. 2015) or cultivated under controlled conditions in laboratory (Kocer et al. 2018, 2020, 2021, 2024; Vehapi et al. 2018). Such studies underscore the broader potential of integrating algal resources into circular bioeconomy strategies alongside terrestrial biomass. However, food-industry residues remain significantly underexplored, despite their high availability, favorable physicochemical properties, and strategic relevance to Turkey's national sustainability goals. Moreover, existing reviews rarely apply systematic decision-support methods such as the Simple Additive Weighting (SAW) within a Multi-Criteria Decision Analysis (MCDA) framework to quantitatively score and rank residue–application alignments.

This study therefore positions Turkey as a region-specific case context for the development of a review-informed, first-stage MCDA screening framework for the biochar valorization of underutilised food-processing residues. Building on gaps in the existing literature, the manuscript (i) compiles and synthesizes physicochemical evidence for ten selected residues, (ii) qualitatively relates these characteristics to suitable thermochemical conversion pathways, (iii) links residue characteristics to application-oriented biochar functions, and (iv) translates these evidence streams into a transparent SAW–WSM-based prioritization structure. Accordingly, the main contribution is not a definitive performance ranking, but a transferable decision-support framework for first-stage residue-to-application screening that can support subsequent validation through targeted experiments, techno-economic assessment, life-cycle analysis, and deployment-specific planning.

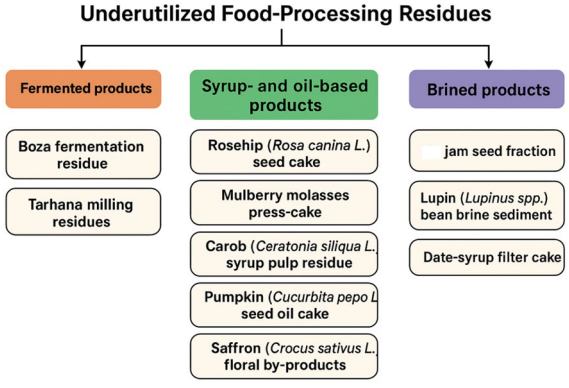


Fig. 1 Categorization of ten underutilized food-processing residues by processing origin

Methodology

Data collection and residue selection

The analysis focused on ten underutilised food-processing residues, broadly grouped into three categories based on their origin and processing method—fermented products, syrup- and oil-based products, and brining-derived products—as illustrated in Fig. 1. Relevant literature was identified through targeted keyword searches in Web of Science, Scopus, ScienceDirect and Google Scholar, using combinations of terms related to biochar, pyrolysis, thermochemical conversion, food-processing wastes and the specific names of the ten residues. The detailed methodological steps are summarised in Fig. 2.

Modelling procedure (SAW–WSM framework)

The suitability of each food-processing residue for different biochar applications was assessed using the SAW method, a well-established WSM within MCDA (Belton and Stewart 2012; Triantaphyllou 2000; Tzeng and Huang 2011). Because residue properties differ in units and scales, all variables were normalised using the linear min–max transformation (Eq. 1), which rescales values to 0–1 based on observed minima and maxima (Eq. 1a), a standard practice in SAW studies (Taherdoost 2023; Tzeng and Huang 2011; Vafaei et al. 2016, 2022). Performance-enhancing variables (e.g., HHV, minerals) and performance-reducing ones (e.g., ash) were treated through benefit- or cost-type normalisation. Cost-type indicators were converted via the inverted min–max form (Eq. 2), and the final normalised indicator followed the appropriate rule for each property (Eq. 3). Normalised variables were grouped into mechanistic proxies for fuel quality, nutrient release, an adsorption-oriented screening proxy, and AD compatibility using monotonic aggregation (Eq. 4), with proxy scores bounded between 0 and 1 (Eq. 4a). Such composite indicators follow hierarchical value modelling in multi-criteria analysis (Belton and Stewart 2012; Triantaphyllou 2000).

Proxy weights for each application were assigned and normalised to sum to one. When a proxy was missing, remaining weights were re-scaled using Eq. 5 to maintain the unity constraint (Eq. 5b), consistent with additive value models applied to incomplete criteria sets [2,3].

Final suitability for residue i in application α was obtained through the weighted sum of proxy scores (Eq. 6), giving values in the range 0–1 (Eq. 6a). These were converted to a 0–100 index using Eq. 7 to aid interpretation while preserving residue ranking (Taherdoost 2023).

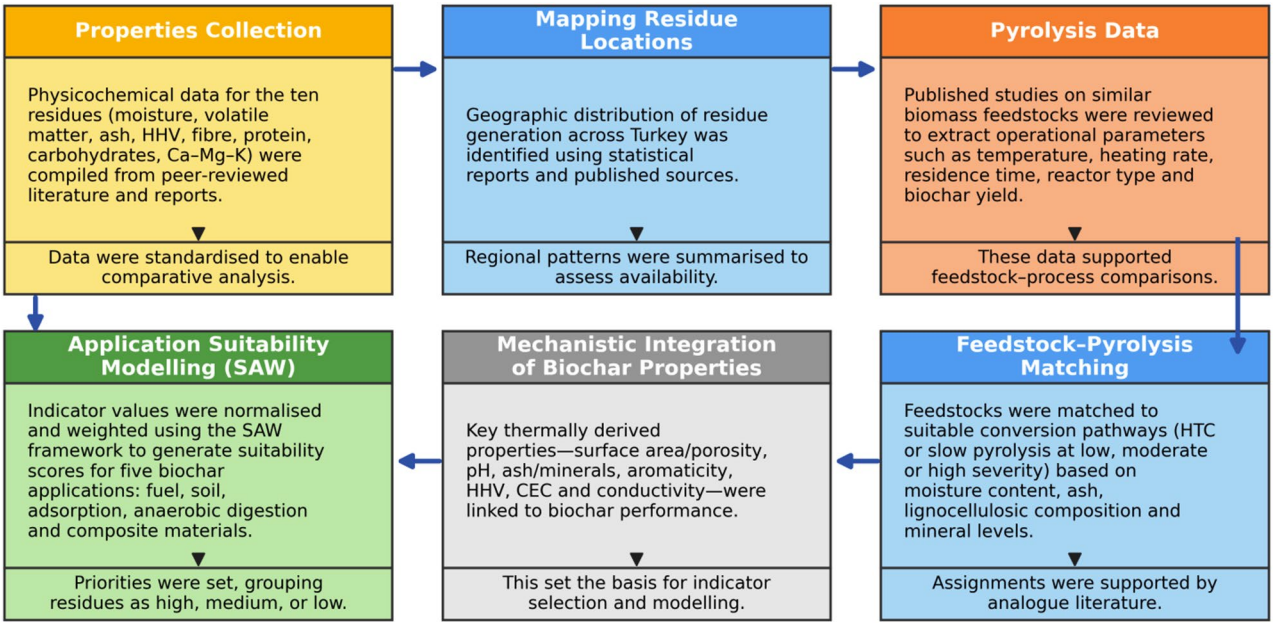


Fig. 2 Methodological workflow for residue evaluation, pyrolysis assessment, and SAW-based suitability modelling

Table 1 Construction of mechanistic proxy criteria from effective normalized indicators

Proxy criterion (K)	Inputs (effective normalised indicators ($\hat{x}_{ij}$))	Benefit/cost designation (handled via Eq. 3)	Proxy definition (arithmetic mean
Fuel quality (FuelQ)	Moisture content (MC), Ash, Higher heating value (HHV)	MC = cost; Ash = cost; HHV = benefit	$z_{i,\mathrm{FuelQ}} = \frac{\hat{x}_{i,\mathrm{MC}} + \hat{x}_{i,\mathrm{Ash}} + \hat{x}_{i,\ \mathrm{HHV}}}{3}$
Nutrient release (Nutrient)	Ca, Mg, K	Ca, Mg, K = benefit	$z_{i,\mathrm{Nutrient}} = \frac{\hat{x}_{i,\mathrm{Ca}} + \hat{x}_{i,\mathrm{Mg}} + \hat{x}_{i,\ \mathrm{K}}}{3}$
Adsorption-oriented screening proxy (Adsorption)	Ash, Dietary fibre (Fibre)	Ash = cost; Fibre = benefit	$z_{i,\mathrm{Adsorption}} = \frac{\hat{x}_{i,\mathrm{Ash}} + \hat{x}_{i,\mathrm{Fibre}}}{2}$
AD compatibility (AD)	Total sugars/carbohydrates (Carb), Protein	Carb, Protein = benefit	$z_{i,\mathrm{AD}} = \frac{\hat{x}_{i,\mathrm{Carb}} + \hat{x}_{i,\mathrm{Protein}}}{2}$

For each proxy, the benefit/cost designation determines whether $\hat{x}_{ij}$ is set to $\tilde{x}_{ij}$ or $\tilde{x}_{ij}^{(inv)}$ (Eq. 3), so that higher z_{ik} always indicates higher suitability

The mapping between physicochemical variables and mechanistic proxies is summarised in Supplementary File 1 (Table S1), while the application-specific proxy weights and their normalised values are provided in Supplementary File 2 (Table S2).

$$\tilde{x}_{ij} = \frac{x_{ij} - x_j^{min}}{x_j^{max} - x_j^{min}} \tag{1}$$

$$x_j^{min} = \min_i x_j, \quad x_j^{max} = \max_i x_j \tag{1a}$$

$$\tilde{x}_{ij}^{(inv)} = 1 - \tilde{x}_{ij} = \frac{x_j^{max} - x_{ij}}{x_j^{max} - x_j^{min}} \tag{2}$$

$$\begin{aligned} \hat{x}_{ij} &= \tilde{x}_{ij}, \text{ if property j is benefit type} \\ \hat{x}_{ij} &= \tilde{x}_{ij}^{(inv)}, \text{ if property j is cost type} \end{aligned} \tag{3}$$

After min–max normalization (Eqs. 1–3), each physicochemical variable is represented by an effective normalized indicator $\hat{x}_{ij} \in |0, 1|$, ensuring that higher values always indicate more favourable performance. Mechanistic proxy scores z_{ik} were then constructed by aggregating selected $\hat{x}_{ij}$ values into four operational proxy criteria representing fuel quality, nutrient release, an adsorption-oriented screening proxy, and AD compatibility (Table 1). Proxy scores were bounded between 0 and 1 (Eq. 4a) and were computed using monotonic aggregation (Eq. 4). Here, $\boldsymbol{fk}(\cdot)$ was implemented as the arithmetic mean of the contributing $\hat{x}_{ij}$ indicators listed in Table 1. Missing inputs were omitted (no imputation) in order to avoid introducing unsupported estimates into the literature-derived dataset; however, because this may

affect cross-residue comparability when indicator coverage differs, the number of available inputs contributing to each residue–proxy score is reported separately in the Supplementary File 1 and reflected through a simple confidence/coverage classification. The adsorption-oriented screening proxy was intentionally defined as a feedstock-level comparative indicator based on dietary fibre (benefit criterion) and ash (cost criterion), rather than as a direct measure of adsorption performance. In this context, dietary fibre was used as a simplified indicator of the structural organic matrix that may support pore development during thermochemical conversion, whereas ash was treated as a counter-indicator because elevated mineral content can reduce the relative carbonaceous fraction and, under some conditions, hinder pore accessibility. This proxy should therefore be interpreted only as a first-pass screening metric and not as a substitute for measured adsorption descriptors such as Brunauer–Emmett–Teller (BET) surface area, pore-size distribution, surface functionality, mineral speciation, or pollutant-specific sorption capacity. More broadly, the proxy structure adopted here is intentionally simplified to preserve transparency, interpretability, and reproducibility at the screening stage; accordingly, the resulting scores are intended for comparative residue-to-application prioritization rather than definitive prediction of real-world biochar performance.

$$z_{ik} = f_k\left(\hat{x}_{ij1}, \hat{x}_{ij2}, \ldots\right) \tag{4}$$

$$0 \le z_{ik} \le 1. \tag{4a}$$

The base weights $w_{\alpha k}$ reflect the dominant drivers of each end-use (adsorption/remediation: adsorption-oriented screening proxy; fuel: fuel quality; soil: nutrient release; AD: AD compatibility), while composite/material use is operationalised by jointly weighting fuel quality and the adsorption-oriented screening proxy (Supplementary File1, Table S2; sensitivity in Section S1.6). Proxy scores are computed using $fk\left(\cdot\right)$ as the arithmetic mean of the contributing $\hat{x}_{ij}$ indicators listed in Table 1; missing inputs are omitted (no imputation), and weights are re-normalized over the available proxy set $K_{i\alpha}$ (Eq. 5).

$$w'_{\alpha k|i} = \frac{w_{\alpha k}}{\sum_{m \in K_{i\alpha}} w_{\alpha m}}, \text{ for } k \in K_{i\alpha} \tag{5}$$

$$K_{i\alpha} \subseteq \{1, \ldots, K\} \tag{5a}$$

$$\sum_{k \in K_{i\alpha}} w'_{\alpha k|i} = 1 \tag{5b}$$

The base weights $w_{\alpha k}$ were assigned to reflect the dominant decision driver in each application domain α. Adsorption/remediation prioritises the adsorption-oriented screening proxy, fuel applications prioritise the fuel-quality proxy, soil amendment prioritises nutrient release, and AD enhancement prioritises AD compatibility, reflecting the dominant performance drivers in each end-use. The adopted base weight matrix is reported in Supplementary File 1, Table S2 and treated as a transparent scenario input.

$$S_{i\alpha} = \sum_{k \in K_{i\alpha}} w'_{\alpha k|i} z_{ik} \tag{6}$$

$$0 \le S_{i\alpha} \le 1 \tag{6a}$$

$$\text{SuitabilityIndex}_{i\alpha} = 100 \times S_{i\alpha} \tag{7}$$

The MCDA structure adopted here is intentionally simplified to preserve transparency, interpretability, and reproducibility at the screening stage; accordingly, its outputs are intended for comparative residue-to-application prioritization rather than definitive prediction of real-world biochar performance.

Characterisation of selected food-processing residues

Property-based differentiation of selected food processing residues for thermochemical valorization

Table 2 provides a systematic comparison of the physicochemical properties of ten underutilized food-processing residues relevant to thermochemical valorization. The dataset spans a wide moisture gradient, from highly aqueous materials such as saffron floral by-product (≈ 90% wet basis), Boza fermentation residue (≈ 70–85%), and lupin brining sediment (≈ 72–80%) to low-moisture residues including fig-jam seed by-product (5.6%) and rosehip seed oil cake (4.4–6.7%), the latter aligning with minimal preprocessing requirements. Ash content also varies substantially, reflecting differences in inherent mineral loads. Lupin brining sediment exhibits the highest ash fraction (≈ 19% dry basis), indicating significant inorganic content, whereas Boza fermentation residue presents the lowest values (0.07–0.50%), indicative of an organics-rich matrix. Pumpkin seed oil cake, carob syrup pulp residue, and saffron floral by-product fall within a mid-range ash band of roughly 3–8%, accompanied by elevated concentrations of agronomically relevant base cations, particularly potassium.

Higher heating values (HHV) range from ~ 14 MJ kg^{-1} in lupin brining sediment to 24–26 MJ kg^{-1} in pumpkin seed oil cake, signifying a substantial spread in energy density. Rosehip seed oil cake and mulberry syrup press-cake also demonstrate elevated HHV values (≈ 18.5–19 MJ kg^{-1}), consistent with their moderate lignin and lipid contents. Dietary fibre is a notable feature

Table 2 Physicochemical profile of food-processing wastes relevant to biochar valorization

Property	Boza fermentation residue	Tarhana residues	Rosehip seed oil cake	Mulberry syrup press-cake	Carob syrup pulp residue	Pumpkin seed oil cake	Saffron floral by-product	Fig-jam seed by-product	Lupin brining sediment	Date syrup filter cake
Moisture content (% (wet basis)	≈ 70–85 (Ayseli et al. 2023; Köse and Yücel 2003)	7.5–17.4 (Kivanc and Funda 2017; Tamer et al. 2007)	4.4–6.7 (Milala et al. 2023)	10–12 (Ta et al. 2023)	7–11 (Kaushik et al. 2025; Tounsi et al. 2017)	6.93 (Budžaki et al. 2018)	89.8 (Criado-Navarro et al. 2024)	5.6 (Nakilcioğlu-taş 2019)	72—80 (Barbeitos 2016)	7.2 (Derouich et al. 2020)
Volatile matter (% (dry basis)	—	79.7% (Głowacki et al. 2022)	63–66 (Ates and Gunduz 2024)	32.3–67.2 (Kaushik et al. 2025)	38.3 (Manis-calco et al. 2021)	79.05 (Petrovič et al. 2024)	10.2 (Fahim et al. 2012)	—	—	69.1 (Oladzad et al. 2024)
Ash (% (dry basis)	0.07–0.50 (Köse and Yücel 2003)	3.7–7.4 (Tamer et al. 2007)	1.9–3.5 (Milala et al. 2023)	2.8 (Ta et al. 2023)	2.8–5.1 (Tounsi et al. 2017; Yousif and Alghzawi 2000)	7.82 (Budžaki et al. 2018)	7.0 (Fahim et al. 2012)	3.17 (Nakilcioğlu-taş 2019)	19 (Parmaki 2022)	2.78 (Sheir 2022)
Protein (% (dry basis)	0.50–1.00 (Yegin and Fernandez Lahore 2012)	8.9–13.6 (Kivanc and Funda 2017; Tamer et al. 2007)	14–15 (Milala et al. 2023)	12.9–21.8 (Li et al. 2017; Ta et al. 2023)	5.8–6 (Tounsi et al. 2017; Yousif and Alghzawi 2000)	38.27 (Budžaki et al. 2018)	10.2 (Fahim et al. 2012)	15.8 (Nakilcioğlu-taş 2019)	1.1 (Barbeitos 2016)	7.4 (Sheir 2022)
Total sugars / carbohydrates (% (dry basis)	10.4–19 (Ayseli et al. 2023; Köse and Yücel 2003)	67.8 (Erbaş et al. 2005)	79 (Cingöz and Şahin 2023)	20.8 (Li et al. 2017)	—	2.74 (Budžaki et al. 2018)	—	56.3 (Nakilcioğlu-taş 2019)	—	66.21 (Sheir 2022)
Dietary fibre (% (dry basis)	—	—	61–67 (Milala et al. 2023)	45.8 (Ta et al. 2023)	47–51 [14]	—	8.8 (Budžaki et al. 2018)	56.6 (Bölek 2021)	—	12.38 (Sheir 2022)
Higher heating value (HHV) (MJ kg^{-1})	—	17.7 (Baslar et al. 2022)	18.5–19 (Ates and Gunduz 2024)	19 (Bora et al. 2024)	18 (Crujeira et al. 2023)	24–26 (Butnaru et al. 2024)	20.2 (Hosseinzaei et al. 2022)	16.8 (Katnić et al. 2022)	14 (Esteves et al. 2020)	—
Calcium (mg 100 g^{-1})	141.4 (Novák et al. 2016)	109 (Daglioğlu 2000)	350–410 (Kizil et al. 2018)	27–113 (Kattil et al. 2024)	608 (Musa Özcan et al. 2007)	155–249 (Sinkovic and Kolmanic 2021)	486 (Hosseini et al. 2018)	18.6–19.0 (Nakilcioğlu-taş 2019)	—	50.2 (Sheir 2022)
Magnesium (mg 100 g^{-1})	59.1 (Novák et al. 2016)	78 (Daglioğlu 2000)	290–320 (Kizil et al. 2018)	39–71 (Kattil et al. 2024)	122 (Musa Özcan et al. 2007)	340–498 (Sinkovic and Kolmanic 2021)	2.93 (Hosseini et al. 2018)	4.6–5.4 (Nakilcioğlu-taş 2019)	—	62.5 (Sheir 2022)
Potassium (mg 100 g^{-1})	14.5 (Novák et al. 2016)	114 (Daglioğlu 2000)	750–820 (Kizil et al. 2018)	194–834 (Kattil et al. 2024)	2720 (Musa Özcan et al. 2007)	780–1220 (Sinkovic and Kolmanic 2021)	542 (Hosseini et al. 2018)	16.7–17.3 (Nakilcioğlu-taş 2019)	—	2.74 (Sheir 2022)

"—" indicates data not reported in the available literature. Because the dataset was compiled from multiple literature sources, full methodological harmonisation was not always possible. Values were extracted on the most comparable reporting basis available, but differences in analytical protocols (e.g., moisture and ash) may contribute to the observed variation. The resulting rankings should therefore be interpreted as screening-level comparisons

in several residues: rosehip seed oil cake (61–67%), fig-jam seed by-product (56.6%), mulberry syrup press-cake (45.8%), and carob syrup pulp residue (47–51%) represent highly lignocellulosic matrices, which are expected to influence char stability and aromaticity. Mineral profiling further underscores substantial variability. Carob syrup pulp residue and pumpkin seed oil cake are particularly enriched in potassium (≈ 2720 mg 100 g^{-1} and up to 1220 mg 100 g^{-1}, respectively), while saffron floral by-product and rosehip seed oil cake show elevated calcium levels (> 350 mg 100 g^{-1}). Collectively, these compositional differences inform the thermal reactivity, carbon



Fig. 3 Geographic distribution of food processing residues for biochar production in Turkey

retention, and post-conversion characteristics of the resulting biochars.

Geographic distribution and regional clustering of selected feedstock

Figure 3 overlays Turkey's provincial boundaries with directional markers indicating the primary regions of production or processing for each of the ten under-researched food processing residues. Boza fermentation residue is distributed across beverage-manufacturing hubs including İstanbul, Ankara, and Eskişehir (Feyiz 2021), while Tarhana milling fines are concentrated in Kahramanmaraş and Isparta (Coşkun 2014; Şekkeli et al. 2015); Rosehip seed cake follows a tri-provincial distribution encompassing Isparta, Erzurum, and Gümüşhane (Kültür and Erarslan 2023). Mulberry syrup press-cake aligns with the fruit-syrup corridor of Malatya and Elazığ (Ozrenk et al. 2010), and Carob syrup pulp residue traces the Mediterranean coastline across Mersin, Antalya, and Adana (Şahin and Taşlıgil 2016). Pumpkin seed oil cake**,** a protein-rich residue, is regionally associated with Konya and Eskişehir (Ermiş and Yanmaz 2022), whereas Saffron floral by-products are geographically unique to Karabük (Safranbolu) (Ege et al. 2020). Fig-jam seed fractions are predominantly generated in Aydın (Piga et al. 2022) and Lupin bean brining sediment is localized in the central agricultural zone of Konya (Ertaş and Bilgiçli 2014). Furthermore, Date-syrup filter cake emerges from the nascent date-processing hub in Şanlıurfa (Paulette 2024).

This geographic mapping reveals both logistical clusters (e.g., carob residues along the southern coast) and more spatially dispersed processing zones (e.g., mulberry and date by-products in eastern and southeastern Turkey), as well as single-province niches (e.g., saffron in Karabük, fig in Aydın, lupin in Konya), which are relevant to the conceptual design of tailored valorization pathways. More cautiously, the clustering of residues points to a potential future planning basis for decentralised biochar hubs: co-located residue streams may reduce transport distance and handling burdens (especially for high-moisture materials), improve supply stability through multi-feedstock aggregation, and enable shared pre-processing and conversion infrastructure. For example, the Mediterranean coastal cluster (carob across Mersin–Antalya–Adana, with nearby agro-industrial corridors) may represent a candidate region for further assessment of decentralised biochar production, while the central Anatolia cluster (pumpkin in Konya/Eskişehir and lupin in Konya) may warrant similar exploratory consideration around existing agricultural processing zones. In contrast, highly localised residues (e.g., saffron in Karabük, fig in Aydın) may be more appropriately explored through micro-scale units and community-based circular-economy pilots. These spatial insights do not replace techno-economic assessment (TEA), life-cycle assessment (LCA), or detailed logistics analysis; rather, they provide a preliminary screening layer for identifying candidate regions and supply-radius considerations for future system-level evaluation.

Process fundamentals

Pyrolysis is a thermochemical process that decomposes biomass into three main products: solid biochar, liquid bio-oil, and non-condensable gases, under limited oxygen conditions. For biochar-focused applications, slow pyrolysis is preferred due to its ability to retain more carbon. It typically operates at 300 to 700 °C, with heating rates of 0.1 to 1 °C per second and residence times of 10 to 100 min (Guo 2020; Özçimen and Ersoy-Meriçboyu 2008; Özyurtkan et al. 2008; Pahnila et al. 2023; Talwar

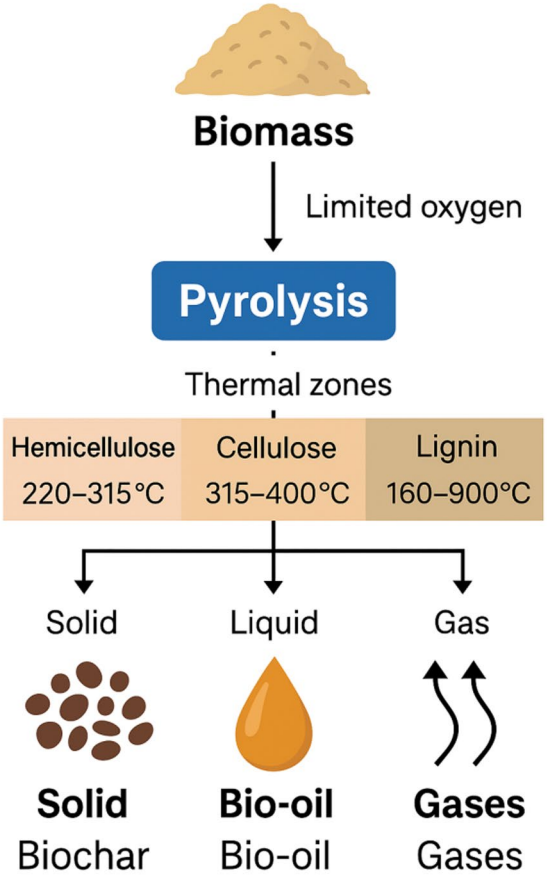


Fig. 4 Schematic of lignocellulosic pyrolysis and resulting product phases

et al. 2025). The thermal degradation of lignocellulose proceeds sequentially based on polymer stability. Hemicellulose decomposes between 220 and 315 °C, cellulose between 315 and 400 °C, while lignin breaks down across a broader range from 160 to 900 °C (Huang et al. 2015; Raza et al. 2021; Yang et al. 2007). These reactions generate volatile products including organic acids, sugars, and phenolic compounds. Extended vapour residence encourages secondary reactions such as tar cracking and repolymerization, which enrich the resulting char in fixed carbon and aromatic structures (Altıkat et al. 2024; Bielecki and Zubkova 2023; Kim and Park 2020; Lu and Gu 2022; Özçimen et al. 2018; Pahnila et al. 2023). In contrast, fast and flash pyrolysis involve higher heating rates (above 10 °C per second) and shorter residence times (milliseconds to seconds), favouring liquid or gas production at the expense of char yield and stability (Halalsheh et al. 2024; Özçimen 2013; Raza et al. 2021; Sun et al. 2017; Tomczyk et al. 2020; Wang et al. 2020). A simplified schematic of pyrolysis zones, thermal ranges, and product pathways is presented in Fig. 4.

Table 3 Comparative analysis of thermal processing routes for biochar production

Process type	Operating temperature (°C)	External heating rate	Residence time	Char Yield (wt %)	References
Torrefaction	280	5 °C min^{-1}	30 min	70	Romão and Conte (2021)
Slow pyrolysis	450	10 °C min^{-1}	30 min	35.5	Yan et al. (2011)
Intermediate pyrolysis	350	200 °C min^{-1}	10 min	55.7	Morgano et al. (2018)
Fast pyrolysis	450	~400 °C s^{-1}	1.4 s	8.4	Morgan et al. (2015)
Flash pyrolysis	500	10,000 °C s^{-1}	0.8 s	5	Hoekstra et al. (2012)
Hydropyrolysis	400 °C (30 bar H_2)	-	-	37.4	Balaguru-murthy et al. (2015)
Microwave-assisted pyrolysis (MAP)	348 ± 34 °C	24.5 ± 4.9 °C min^{-1}	60 min	40	Wallace et al. (2019)
Catalytic pyrolysis	500		60 min	12	Yildiz et al. (2015)
Plasma pyrolysis	900			61.20	Tang and Huang (2005)
Vacuum pyrolysis	300 (10 kPa)	15 °C min^{-1}	60 min	41.8	Ozbay and Ayrilmis (2017)

Table 3 distils the rich diversity of biomass-to-biochar thermochemical routes into ten clearly defined pyrolysis regimes. Each process type occupies its own kinetic "window," distinguished by characteristic temperature, heating-rate and vapour-residence combinations that steer product distributions toward solid carbon, liquid bio-oil or syngas. From low-temperature torrefaction and char-favouring slow pyrolysis, through liquid-centred fast, flash and vacuum variants, to advanced options such as hydropyrolysis, microwave-assisted, catalytic and plasma systems, the table underscores how subtle shifts in operating parameters create markedly different pathways and end-use opportunities. These classifications provide a practical framework for selecting or designing reactors that deliver the desired balance of biochar quality, energy efficiency and downstream processing compatibility.

Application-oriented evidence of biochar utility across energy, environmental, and agricultural sectors

The practical deployment of biochar has evolved from conceptual validation to a multidimensional strategy for addressing critical challenges in energy production,

Table 4 Summary of representative performance metrics for biochar applications

Application category	Representative findings
Energy carrier and combustion co-firing Higher heating value Hardgrove Grindability Index	Torrefaction of vine-pruning residues at 400 °C for 30 min increased the higher heating value from 18.6 to 29.8 MJ kg^{-1} (Nunes et al. 2021) Agro-forestry-waste chars torrefied at 280–320 °C show a Hardgrove Grindability Index of 30 to 55, consistent with easily pulverised coals (Nunes 2020)
Soil amendment and carbon sequestration Soil pH Cation-exchange capacity Field crop yield	In a short-term field experiment in Oklahoma, Omara et al. (2023) evaluated the combined application of 10 t ha^{-1} hardwood biochar and 120 kg N ha^{-1} at two contrasting sites. On the coarse-textured Lake Carl Blackwell sandy-loam plot, soil pH increased from 5.7 to 6.2 and the cation-exchange capacity (CEC) rose by 16% relative to the nitrogen-only control. At the finer-textured Efaw clay-loam site, pH rose from 5.6 to 6.1 and CEC improved by 4%. When results were averaged across both locations, the biochar + N treatment delivered a mean CEC gain of 10% and a 0.4-unit elevation in pH within a single growing season (Omara et al. 2023)
Water and wastewater treatment Maximum adsorption capacity Specific surface area	Cotton-derived magnetic biochar (Fe_xO_y–BC) produced at 700 °C achieved a Langmuir adsorption capacity of 252.7 mg g^{-1} for Pb^{2+} and retained at least 95% of this capacity after five regeneration cycles (Yao et al. 2025) Wang et al. (2024) reported Langmuir capacities of 224.77 mg g^{-1} for Pb^{2+} and 400.11 mg g^{-1} for ciprofloxacin for the $CoFe_2O_4$/N,S-biochar adsorbent in single-component systems (Wang et al. 2024) Dang et al. (2023) lists a BET surface area of 1 196 m^2 g^{-1} and a Langmuir capacity of 359.7 mg g^{-1} for methylene blue on the KOH/NaOH-activated rice-husk biochar
Anaerobic digestion Cumulative methane yield – high-nitrogen substrate	In a high-nitrogen chicken-manure digester, dosing 5% (v/v) acid–alkali-treated wood biochar elevated cumulative methane production from 46 mL CH_4 g^{-1} VS in the untreated control to 399 mL CH_4 g^{-1} VS, representing an 8.7-fold increase. The same amendment lowered total ammonium-nitrogen from 4418 to 2478 mg L^{-1}—a 44% reduction—thereby mitigating total ammonium nitrogen (TAN) inhibition (Ngo et al. 2024) Co-pyrolysis biochar prepared from a 1:1 mixture of digestate and rice straw and dosed at 1.5 g L^{-1} to food-waste digesters raised the cumulative methane yield from 114 ± 11 mL CH_4 g^{-1} VS (control) to 156 ± 7 mL CH_4 g^{-1} VS, a 37% increase. Microbial analyses showed selective enrichment of *Methanosarcina* and other DIET-capable taxa, indicating that the yield gain is linked to enhanced direct interspecies electron transfer (Yang et al. 2025)
Electro-materials and catalysis Oxygen-reduction reaction activity Specific capacitance Capacitive-de-ionisation performance	Microwave-assisted activation of mixed food-waste yielded a three-dimensional carbon aerogel that delivered a specific capacitance of 314 F g^{-1} at 1 A g^{-1} and retained > 90% of that value after 10 000 charge–discharge cycles (Dong et al. 2025) Porous carbon produced from corn cobs (CBC-800) reached a salt-adsorption capacity of 19.2 mg g^{-1} in 3 g L^{-1} NaCl at 1.2 V, outperforming conventional activated carbon under the same conditions (Wang et al. 2023)
Emerging structural and thermal uses Mechanical strength of cement composites Latent-heat retention in phase-change materials	Replacing 5 wt % of Portland cement with sugar-cane-bagasse biochar (water-to-cement ratio = 0.35) raised the 28-day compressive strength of paste specimens by 48% and refined capillary porosity, as confirmed by scanning electron microscopy/energy-dispersive spectroscopy (SEM/EDS) imaging (Paula et al. 2025) A shape-stable composite prepared by vacuum-impregnating palmitic acid into KOH-activated garlic-peel porous carbon retained a melting enthalpy of 52.5 J g^{-1} and lost < 1.5% of its latent heat after 200 melt–freeze cycles (Gao et al. 2023)

environmental protection, agricultural productivity, and materials development. As a structurally and chemically tunable carbonaceous solid, biochar's functional performance is inherently dictated by its physicochemical properties, which can be deliberately engineered through feedstock selection, pyrolysis parameters, and post-treatments. As summarized in Table 4, the current application landscape emphasizes not a one-size-fits-all approach, but the strategic alignment of biochar attributes with sector-specific requirements.

In energy applications, biochars that undergo thermal treatment, particularly through torrefaction, show improved energy content and are easier to grind. These enhancements make them promising candidates for direct combustion or blending with fossil fuels. For example, treating vine-pruning waste at 400 °C through torrefaction raised its higher heating value significantly, from 18.6 to 29.8 MJ per kilogram (Nunes et al. 2021), while agro-forestry waste biochars achieved Hardgrove Grindability Index values consistent with coal-like performance (Nunes 2020). These modifications enable integration into existing thermal conversion systems with minimal retrofitting. For soil amendment and carbon sequestration, biochar contributes to improved soil health through elevation of pH, enhancement of cation-exchange capacity (CEC), and increased nutrient retention (Karakaş et al. 2017). A short-term field trial in Oklahoma demonstrated that hardwood biochar application increased CEC by up to 16% and raised soil pH by 0.4 units, effects that were consistent across coarse- and fine-textured soils (Omara et al. 2023). Such properties are crucial for sustaining crop yields and enhancing the long-term carbon sink capacity of agricultural soils.

In water and wastewater treatment, surface-engineered biochars, especially those modified with magnetic materials or through chemical activation, have shown outstanding adsorption performance. For example, magnetic biochar made from cotton waste achieved a Langmuir adsorption capacity of 252.7 mg g^{-1} for lead ions (Pb^{2+}) and maintained over 95% efficiency even after several reuse cycles (Yao et al. 2025), while other biochars doped with heteroatoms exhibited similarly high affinities for

both heavy metals and pharmaceuticals (Dang et al. 2023; Wang et al. 2024). These materials rival, and in some cases outperform, conventional activated carbons. In anaerobic digestion systems, biochar serves dual functions: as a microbial support matrix and as a buffer for inhibitory compounds. In high-nitrogen chicken-manure digesters, biochar dosing raised cumulative methane yields by nearly 8.7-fold and reduced total ammonium nitrogen concentrations by 44% (Ngo et al. 2024). Co-pyrolysed biochar from digestate and rice straw further enhanced methane production while selectively enriching for electroactive microbial consortia (Yang et al. 2025), demonstrating the role of biochar in facilitating direct interspecies electron transfer (DIET).

The use of biochar in electrochemical and catalytic systems is gaining prominence due to its high specific surface area, electrical conductivity, and structural stability. Biochar-based aerogels derived from food waste have delivered specific capacitances exceeding 300 F g^{-1} with remarkable cycling stability (Dong et al. 2025). Additionally, porous carbon from corn cobs has shown superior salt adsorption performance in capacitive deionisation setups compared to commercial activated carbon (Wang et al. 2023). In structural and thermal applications, biochar is emerging as a multifunctional additive. Substitution of 5 wt% of cement with sugarcane bagasse biochar resulted in a 48% increase in compressive strength and refined pore architecture (Paula et al. 2025). Similarly, KOH-activated garlic peel biochar impregnated with palmitic acid retained over 98.5% of its latent heat capacity after 200 thermal cycles, confirming its suitability in phase-change energy storage materials (Gao et al. 2023).

Mechanistic integration of biochar properties with functional performance

As biochar technology has advanced, the focus has moved beyond simply asking whether it works to understanding how and under what conditions it performs best. Recent studies indicate that the effectiveness of a specific biochar depends on a combination of physicochemical properties shaped during thermal conversion and any subsequent treatments. As illustrated in Fig. 5, this section brings together mechanistic insights and peer-reviewed findings to connect seven key properties:

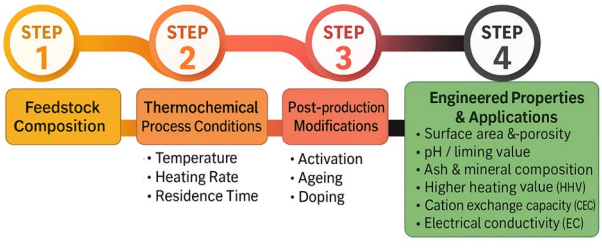


Fig. 5 Framework linking biochar inputs, properties, and end-uses

surface area and porosity, pH, ash and mineral composition, aromaticity (fixed carbon), higher heating value (HHV), cation-exchange capacity (CEC), and electrical conductivity (EC), with their most appropriate applications. The aim is to offer a property-focused framework that can guide both production strategies and regulatory standards in areas such as climate-smart agriculture, environmental remediation, and energy systems.

Biochar is increasingly recognized as a tunable functional material, whose physicochemical properties can be strategically engineered to fulfill specific performance objectives. The resulting property spectrum is governed by three primary and controllable factors: (i) the intrinsic composition of the feedstock (He et al. 2024; Xu et al. 2022), which defines the baseline inventory of organic compounds and mineral constituents; (ii) the parameters of the thermochemical conversion process (Cárdenas-Aguiar et al. 2024; Sharma et al. 2024)—including peak temperature, heating rate, residence time, and processing atmosphere—which influence structural and chemical transformations; and (iii) post-production modifications (Sajjadi et al. 2019) such as physical or chemical activation, environmental ageing (Liu et al. 2024, 2021), and heteroatom doping (Chandrasekar et al. 2024), which can further tailor surface reactivity and functionality. The subsequent sub-sections synthesize the mechanistic pathways through which these variables shape seven critical biochar properties that underpin its effectiveness across a broad range of high-value applications.

To strengthen the connection between this mechanistic framework and the ten residues evaluated in this review, Table 5 provides illustrative "example residues" selected directly from the feedstock property dataset (Table 2). Each of these properties is linked to (i) its most relevant application domains, (ii) feedstock characteristics that favour its development, (iii) optimised pyrolysis or thermochemical conditions, and (iv) optional post-treatment strategies for enhancement. For example, chars with high BET surface area and functional group density are well-suited for aqueous pollutant adsorption and energy storage; those with high HHV and structural carbon are valuable as renewable solid fuels or reductants; and alkaline, mineral-rich chars demonstrate efficacy as liming agents and nutrient sources in degraded or acidic soils. This integrative framework provides a foundation for rational design of biochar materials, wherein production parameters are deliberately tuned to yield performance-optimised products for specific end-uses. It also supports the development of application-driven characterisation protocols and regulatory standards aligned with biochar's role in climate-resilient agriculture, environmental remediation, and low-carbon energy systems.

Table 5 Mechanistic alignment of biochar properties with application domains and enabling factors

	Biochar property (primary metric)	Applications that benefit most	Feedstock traits that favor the property	Optimized process conditions	Post-treatments for enhancement	Example residues (selected using Table 1 proxies)
1	Surface area & hierarchical porosity (BET, pore-size distribution)	Aqueous/soil adsorption of heavy metals & organics High-power supercapacitor carbons (Inyang et al. 2012; Mahmood et al. 2025)	Precursors with low ash content and fibrous or cellulose-rich structures promote microporous matrix formation (Román et al. 2017)	Stepwise temperature elevation enhances micro- and mesoporosity until excessive heat begins pore collapse (Chatterjee et al. 2020)	Physical activation using steam or CO_2 broadens pore volume and improves pore uniformity (Lua and Guo 2000; Molina-Sabio and Rodrıguez-Reinoso 2004)	Rosehip seed oil cake; Fig-jam seed by-product; Carob syrup pulp residue
2	pH / liming potential (initial char pH, carbonate alkalinity)	Amendment of acid Ferralsols & Ultisols Crop-yield enhancement Acid-mine-tailing reclamation (Agegnehu et al. 2016; Cornelissen et al. 2018; Gómez et al. 2021)	Biomass containing alkaline-forming elements (e.g., Ca, Mg, K) supports intrinsic liming potential (Singh 2006)	Mild pyrolysis preserves these mineral phases, yielding higher liming efficiency than more severe treatments (Gaskin et al. 2008)	Co-application with agricultural lime can synergistically improve pH buffering in acid soils (Iticha et al. 2024)	Carob syrup pulp residue; Pumpkin seed oil cake; Rosehip seed oil cake
3	Ash & mineral speciation (K, Ca, Mg, P; alkali and alkaline earth metals, AAEMs)	Slow-release fertiliser In-situ catalyst in pyrolysis/gasifier reactors Filler for polymer composites (Aboughaly et al. 2023; Limwikran et al. 2018; Shen et al. 2015)	Feedstocks rich in plant-available nutrients but low in siliceous impurities yield beneficial mineral profiles in biochar (Naeem et al. 2014; Nguyen et al. 2020)	Gentle pyrolysis better retains soluble nutrient forms, while harsher conditions convert them into less bioavailable phases (Bilias et al. 2023)	Ultrasound-assisted acid washing selectively removes excess ash while preserving essential nutrient elements (Lima et al. 2021; Taylor et al. 2020)	Lupin brining sediment; Pumpkin seed oil cake; Saffron floral by-product; Tarhana residues
4	Aromaticity / fixed-carbon fraction (O:C < 0.2	Carbon-offset & trading schemes Long-term reclamation layers (De Gryze et al. 2010; Spokas 2010; Thi et al. 2021)	Feedstocks with high aromatic precursor content favour the formation of condensed polyaromatic structures for long-term stability (Kopp Alves et al. 2024; Nan et al. 2023)	Higher pyrolysis temperatures reduce H/C and O/C ratios, enhancing the fixed-carbon content and aromaticity of the biochar (Liu et al. 2018; Xiao et al. 2016)	High-temperature annealing post-pyrolysis improves structural ordering without sacrificing recalcitrance (Giorcelli et al. 2021; Harvey et al. 2012)	Rosehip seed oil cake; Fig-jam seed by-product; Carob syrup pulp residue
5	Higher heating value (HHV) (MJ kg^{-1})	Briquettes & pellets Biomass–coal co-firing Small-scale metallurgical reductant (García et al. 2021; Kosakowski et al. 2020)	Carbon-dense, oxygen-lean biomass yields energy-rich chars suitable for fuel applications (Kosakowski et al. 2020; Qian et al. 2020)	Moderate-to-high temperature pyrolysis increases fixed carbon proportion and energy density (Angın 2013)	Briquetting or densification improves volumetric HHV and combustion efficiency (Ngene et al. 2024; Reis Portilho et al. 2020)	Pumpkin seed oil cake; Saffron floral by-product; Mulberry syrup press-cake; Rosehip seed oil cake
6	Cation-exchange capacity (CEC)	Fertiliser-efficiency booster on coarse soils Rehabilitation of degraded lands (Ndibize et al. 2022; Singh et al. 2022)	Biomass rich in carboxylic and phenolic groups enables the formation of chars with high surface reactivity and nutrient retention (Lago et al. 2021; Yuan and Xu 2011)	Lower pyrolysis temperatures preserve oxygenated functional groups essential for cation exchange (Banik et al. 2018; Gai et al. 2014)	Hydrogen peroxide oxidation increases surface acidity and enhances ammonium and cation sorption capacities (Huff and Lee 2016; Wang et al. 2015)	Tarhana residues; Mulberry syrup press-cake; Boza fermentation residue; Date syrup filter cake
7	Electrical conductivity	Anaerobic digestion & methanogenesis Microbial fuel cells Capacitive de-ionisation (Mishra et al. 2024; Shim and Patel 2024; Valentin et al. 2023)	Aromatic-rich precursors containing trace metals support the formation of conductive graphitic domains (Demir et al. 2015; Xia et al. 2022)	High-temperature pyrolysis promotes turbostratic stacking and electron mobility through the carbon matrix (Gabhi et al. 2020; Giorcelli et al. 2021)	Post-pyrolysis graphitisation or metal-assisted carbon structuring can significantly enhance conductivity (Giorcelli et al. 2021; Xia et al. 2022)	Carob syrup pulp residue; Pumpkin seed oil cake; Lupin brining sediment; Saffron floral by-product

Pyrolysis strategy and process matching

The strategic alignment of pyrolysis conditions with feedstock characteristics is critical to achieving reproducible and functionally targeted biochar outputs. The routing of the ten residues across the thermochemical pathways in Fig. 6 is essentially a translation of composition into process windows. Moisture content, ash level, fibre and lignin fractions, and macro-mineral load jointly determine whether a feedstock is better aligned with hydrothermal carbonization (HTC) or with low-, moderate-, or high-severity slow pyrolysis.

Rosehip seed cake, pumpkin seed oil cake and mulberry syrup press-cake form the driest, most energy-dense subgroup, with low moisture, relatively low ash,

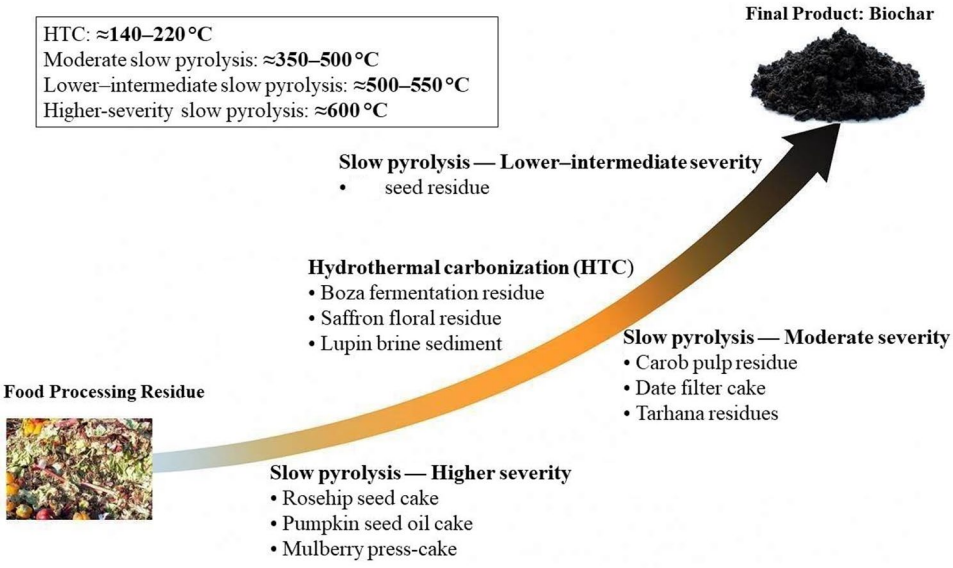


Fig. 6 Thermochemical conversion pathways of food-processing residues to biochar

and substantial lignocellulosic and fixed-carbon content. They are assigned to high-temperature slow pyrolysis or annealing around 600 °C. At this severity, secondary devolatilisation and aromatisation are advanced, producing chars with high fixed-carbon fractions, reduced volatile matter, and elevated higher heating values This routing is consistent with studies on compositionally similar oilseed cakes: for example, safflower seed press cake pyrolysed at 600 °C produced biochar with fixed carbon of about 81% and a higher heating value near 30 MJ kg^{-1}, confirming that lignin-rich oilseed residues respond favourably to this high-severity window (Angın, 2013). Similar behaviour has been reported for other oilseed and lignocellulosic residues. Rapeseed cake, maize cobs and walnut shells slow-pyrolysed at 600 °C yield carbon-rich chars. Seed-cake systems such as rapeseed, walnut, hemp, pumpkin, flax and sunflower likewise show increasing HHV and fixed-carbon content as treatment temperatures approach 600 °C (Sieradzka et al. 2025). Hemp-stalk biochars carbonised at 400–600 °C are classified as solid biofuels due to their low moisture and volatile matter, limited ash and high carbon content, while broader agro-food waste studies confirm that 600 °C chars exhibit the lowest H/C and O/C ratios and the strongest aromatic condensation (Marrot et al. 2022). Taken together, these analogue systems support the assignment of rosehip seed cake, pumpkin seed oil cake and mulberry syrup press-cake to a high-severity slow-pyrolysis window around 600 °C when the target is long-lived, energy-dense, carbon-rich biochar.

The fig-jam seed fraction, although also a dry and carbon-rich residue, is placed in a slightly milder slow-pyrolysis band (≈ 500–550 °C). This routing is closely supported by work on compositionally similar fruit-seed residues. Date seeds have been converted to biochar by slow pyrolysis at 550 °C for 30 min under nitrogen, yielding a material with a specific surface area of about 307 m^2 g^{-1} (Mihajlović et al. 2025). In parallel, apricot and cornelian cherry seeds have been pyrolysed at 500 °C, a temperature selected as an optimal compromise between biochar stability, calorific value (≈ 31 MJ kg^{-1}) and yield (Saletnik et al. 2025). Taken together, these examples indicate that dry fruit-seed residues perform well when processed in the 500–550 °C slow-pyrolysis window, supporting the assignment of the fig-seed by-product to this lower–intermediate severity band when adsorption-oriented applications are prioritised. Boza fermentation residue, saffron floral by-products and lupin brining sediment occupy the opposite end of the spectrum: they are highly wet and structurally unstable. For such substrates, Fig. 6 assigns HTC as the primary conversion route. This choice is consistent with HTC studies on similarly wet, nutrient-rich wastes. For example, dairy-processing sludge treated by HTC at 160–220 °C for 1 h has been converted into nutrient-rich hydrochars suitable for use as organo-mineral fertilisers (Kwapinska et al. 2023). A similar approach has been applied to brewery residues, where high-moisture spent grains were hydrothermally carbonised at 140–200 °C to produce hydrochars, confirming the suitability of HTC for wet food-industry by-products (Skrzypczak et al. 2024). By analogy, routing boza fermentation residue, saffron floral residues and lupin brining sediment through HTC is a more rational option than forcing them into high-temperature dry pyrolysis after extensive pre-drying.

The remaining residues—carob syrup pulp, date-syrup filter cake and tarhana residues—display intermediate characteristics: their moisture contents are moderate,

Table 6 Feedstock grouping and literature-supported justification for process windows

Residue group	Residues	Recommended process window	Key justifying property trigger (from Table 2)	Supporting analogue evidence
Very wet residues	Boza fermentation residue; Saffron floral by-products; Lupin brining sediment	HTC (≈ 140–220 °C)	High moisture (typically > 80%) makes pre-drying energy-intensive; HTC accommodates wet matrices and avoids extensive drying prior to conversion	HTC of similarly wet residues (dairy-processing sludge 160–220 °C; brewery spent grains 140–200 °C) yielding nutrient-rich hydrochars (Kwapinska et al. 2023; Skrzypczak et al. 2024)
Dry, energy-dense subgroup	Rosehip seed cake; Pumpkin seed oil cake; Mulberry syrup press-cake	High-severity slow pyrolysis / annealing (≈ 600 °C)	Low moisture (≈ 4–12%) with comparatively low–moderate ash and higher HHV/structural carbon → high temperature promotes devolatilisation and aromatisation, yielding carbon-rich, energy-dense chars	Oilseed/lignocellulosic analogues at ~ 600 °C (e.g., safflower press cake at 600 °C; seed-cake systems showing increasing HHV/fixed-C approaching 600 °C; agro-food waste chars at 600 °C showing strongest aromatic condensation) (Angın 2013; Marrot et al. 2022; Sieradzka et al. 2025)
Dry fruit-seed fraction (adsorption-oriented routing)	Fig-jam seed fraction	Lower–intermediate slow pyrolysis (≈ 500–550 °C)	Low moisture (~ 5–6%) and seed-type structure → 500–550 °C provides a screening compromise between stability/HHV/yield while supporting adsorption-oriented deployment	Fruit/date-seed analogues treated in 500–550 °C window (date seeds at 550 °C; apricot/cornelian cherry seeds at ~ 500 °C selected as a compromise for stability/HHV/yield) (Mihajlović et al. 2025; Saletnik et al. 2025)
Intermediate residues	Carob syrup pulp residue; Date-syrup filter cake; Tarhana residues	Moderate-severity slow pyrolysis (≈ 350–500 °C)	Moderate moisture (≈ 7–17%) with appreciable carbohydrates/fibre and non-negligible minerals → moderate temperatures balance deoxygenation with functional-group retention and preserve useful mineral/nutrient features	Analogues supporting moderate-temperature routing: carob pulp 280–400 °C; date-processing by-products 350–550 °C; cereal/starch-rich wastes showing useful compromise at 400–500 °C (Al-Tarawneh 2022; Maniscalco et al. 2021; Wystalska and Kwarciak-Kozłowska 2021)

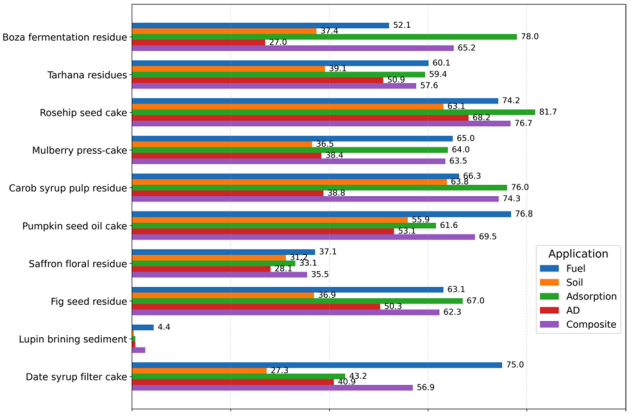


Fig. 7 SAW-based suitability scores across five biochar application domains

they contain appreciable carbohydrates and fibre, and they retain a non-negligible mineral fraction. For such materials, moderate-temperature slow pyrolysis offers a compromise between deoxygenation and functional-group retention. For carob pulp, temperatures between 280 and 400 °C tend to shift the product distribution toward the biochar fraction, with the heating value of the solid phase rising steadily as temperature increases; authors have noted the potential of carob-derived chars in biocomposite applications (Maniscalco et al. 2021). Date seeds and other date-processing by-products have been carbonised in the 350–550 °C range to produce chars that retain appreciable nutrient contents while developing progressively greater porosity (Al-Tarawneh 2022). Biodegradable plant wastes rich in starch and cereals—analogous to the cereal-based tarhana dough—have been pyrolysed at 400, 500, 600 and 700 °C; at 400–500 °C, the resulting biochars show a useful compromise between yield, increasing carbon content, rising pH and the gradual development of surface area (Wystalska and Kwarciak-Kozłowska 2021). Taken together, these analogue systems support the classification of carob pulp residue, date-syrup filter cake and tarhana residues into a moderate-severity slow-pyrolysis window in Fig. 6. To clarify why the temperature bands were selected, Table 6 summarises the residue grouping, the recommended thermochemical window, and the dominant physicochemical trigger (s) underpinning each routing decision, supported by analogue feedstock studies cited in this section.

Application alignment based on modelling results

The SAW-based suitability scores (Fig. 7) quantify how well each of the ten food-processing residues aligns with five major biochar application domains: fuel, soil amendment, adsorption/remediation, anaerobic digestion (AD) enhancement, and composite/material use. Scores range from 0 to 100 and were computed using the modelling procedure described in Section "Modelling procedure (SAW–WSM framework)" and Eqs. (1)– (7). To strengthen integration of the quantitative outputs,

Table 7 Top three residues per application domain based on SuitabilityIndex

Application domain	Top 3 residues (SuitabilityIndex)
Fuel	Pumpkin seed oil cake (76.8); Date syrup filter cake (75.0); Rosehip seed cake (74.2)
Soil amendment	Carob syrup pulp residue (63.8); Rosehip seed cake (63.1); Pumpkin seed oil cake (55.9)
Adsorption/remediation	Rosehip seed cake (81.7); Boza fermentation residue (78.0); Carob syrup pulp residue (76.0)
AD enhancement	Rosehip seed cake (68.2); Pumpkin seed oil cake (53.1); Tarhana residues (50.9)
Composite/material use	Rosehip seed cake (76.7); Carob syrup pulp residue (74.3); Pumpkin seed oil cake (69.5)

Table 7 summarizes the top three residues per application domain with their SuitabilityIndex values. In addition, a radar-chart visualization of multi-domain profiles is provided in the Supplementary File 2 (Fig. S1) to facilitate cross-residue comparison. To provide a limited ground-truth check of the proxy-based ranking, a literature-based validation-anchor table for selected residues or closely related feedstocks has been included in Supplementary File 1 (Section S1.8, Table S5).

Across domains, the composite index (last column in Fig. 7) spans from 2.7 for lupin brining sediment to 76.7 for rosehip seed cake, indicating substantial dispersion in overall suitability under the adopted proxy set and weights. Rosehip seed cake, carob syrup pulp residue, and pumpkin seed oil cake repeatedly appear among the highest-ranked residues across multiple domains, whereas saffron floral residue and lupin brining sediment exhibit low absolute scores even in their best categories. These contrasts should be interpreted as comparative priority signals within the current criteria set; rankings may shift if additional constraints (e.g., logistics, contaminants, regulatory thresholds, or application-specific performance data) are introduced, which is a recognized sensitivity in MCDA-based screening (Äkräs et al. 2022). Repeated high ranking across multiple domains may partly reflect genuine multifunctionality in some residues, but it may also arise from overlap among proxy definitions and shared compositional drivers; accordingly, such patterns should be viewed as screening-level indications of broader potential rather than proof of universal superiority. The final suitability scores represent first-stage screening outputs derived from literature-based feedstock indicators and simplified proxy structures, not evidence that a given residue will necessarily perform well in an experimental biochar application. Because the SAW model is compensatory, high overall scores should not be interpreted as evidence that a residue is uniformly strong across all operational constraints; rather, they indicate relative screening priority under the adopted criteria and weighting assumptions. The domain-wise patterns are interpretable when traced back to the screening proxy definitions (Table 1) and physicochemical inputs (Table 2). The following subsections summarize the principal drivers of high-ranking residues in each application domain.

Fuel applications

For fuel applications, pumpkin seed oil cake (76.8), date syrup filter cake (75.0), and rosehip seed cake (74.2) are the top-ranked residues (Table 7). Accordingly, these residues emerge as the leading candidates for energy-oriented deployment because their rankings are driven by the fuel-quality proxy, which rewards higher HHV (benefit-type) while penalizing moisture and ash burdens (cost-type; inverted during normalization; Eqs. 1–3). Fuel also emerges as the highest-scoring domain for tarhana residues (60.1), mulberry press-cake (65.0), saffron floral residue (37.1), and lupin brining sediment (4.4), whereas Boza fermentation residue (52.1) and fig seed residue (63.1) occupy intermediate values. Importantly, because the fuel index is derived from proximate screening proxies, it does not explicitly represent operational constraints such as ash fusibility, slagging/corrosion propensity, or emission-relevant heteroatom chemistry; accordingly, high-ranked residues are best interpreted as candidates for targeted follow-up testing rather than as stand-alone certification of fuel performance (Agar et al. 2023; Luan et al. 2025). Beyond energy recovery, several residues cluster strongly toward adsorption-oriented deployment, reflected in the high density of adsorption scores above 60.

Adsorption and remediation applications

Adsorption/remediation exhibits the densest cluster of high scores (Fig. 7), with rosehip seed cake (81.7), Boza fermentation residue (78.0), and carob syrup pulp residue (76.0) forming the top three (Table 7), followed by fig seed residue (67.0), mulberry press-cake (64.0), and pumpkin seed oil cake (61.6). This clustering is consistent with the formulation of the adsorption-oriented screening proxy, which aggregates mineral- and structure-related feedstock indicators available in the compiled dataset as first-pass screening surrogates (Table 1). However, adsorption performance is inherently application-specific and is governed by post-pyrolysis properties such as biochar surface area, pore architecture (including pore-size distribution), surface chemistry/functional groups, and mineral phases; therefore, these results are presented as comparative screening outputs that should be complemented, where possible, by adsorption isotherms and kinetics together with Brunauer–Emmett–Teller (BET) surface-area and pore-size analysis and

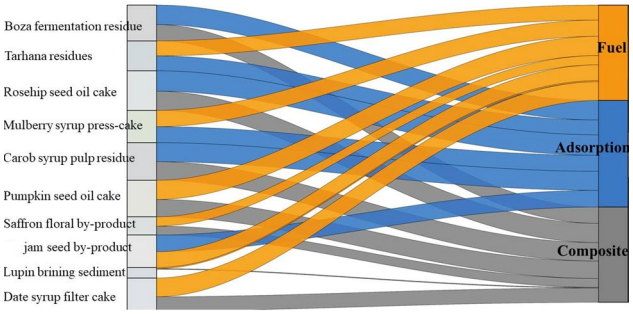


Fig. 8 Top-priority and second-best biochar applications for each residue

surface-chemistry characterization (Tan et al. 2021). Relative to adsorption, soil amendment and AD enhancement display more moderate score ranges, but their rankings remain informative for deployment planning and co-benefit positioning.

Soil amendment applications

For soil-oriented deployment, carob syrup pulp residue (63.8), rosehip seed cake (63.1), and pumpkin seed oil cake (55.9) are the highest-ranked residues (Table 7). Their elevated scores are driven by the nutrient-release proxy, which weights macro-mineral contributions (Ca, Mg, and K) aggregated from Table 2 and applies the adopted soil-deployment weighting scheme (Supplementary Table S2). Because agronomic outcomes can also depend on pH/liming value, salinity, contaminant constraints, and ageing effects, the soil SuitabilityIndex is interpreted here as a nutrient-oriented prioritization indicator rather than a direct predictor of yield response.

Anaerobic digestion enhancement

In the AD enhancement domain, rosehip seed cake ranks first (68.2), followed by pumpkin seed oil cake (53.1) and tarhana residues (50.9) (Table 7), with fig seed residue close behind (50.3). These rankings reflect the AD-compatibility proxy emphasizing carbohydrate and protein indicators (Tables 1, 2). While AD is not the single top-ranked application for most residues, the score distribution suggests that several residues remain plausible co-substrates or additive candidates in digesters, particularly where stabilization, micronutrient supply, or biochar-mediated process enhancement is targeted. However, the AD-oriented score does not explicitly capture measured methane yield, biodegradability, inhibition effects, digestate quality, or reactor-specific operating conditions; it should therefore be interpreted as a screening indicator rather than a direct predictor of digester performance. To translate the domain-wise scores into actionable pathways, Fig. 8 summarizes the top-priority and second-best application for each residue.

Composite and materials use, and top-two deployment pathways

Figure 8 consolidates residue-specific deployment options by reporting the highest and second-highest SAW scores per residue. Boza fermentation residue is best aligned with adsorption (78.0), with composites/material use (65.2) as the second-ranked option. Tarhana residues favor fuel (60.1) with adsorption (59.4) close behind. Rosehip seed cake and carob syrup pulp residue both rank highest for adsorption (81.7 and 76.0, respectively), with composites/material use as the second-best option (76.7 and 74.3), indicating multi-domain versatility. Similarly, the composite/material suitability scores do not directly capture interfacial compatibility, mechanical performance, thermal stability, or processing requirements; they should therefore be interpreted as comparative screening outputs rather than direct evidence of materials performance. In contrast, lupin brining sediment exhibits low absolute scores across domains (fuel 4.4; composites 2.7), indicating weak comparative advantage within the present proxy-and-weight framework and suggesting that blending, alternative pre-treatment, or non-biochar valorization routes may be more appropriate within the current decision space.

Taken together, the composite index, domain-wise rankings, and top-two pathways support a pragmatic prioritization into three clusters: (i) high-priority residues (rosehip seed cake, carob syrup pulp residue, pumpkin seed oil cake) with consistently strong suitability across adsorption, fuel, and composites and comparatively stronger potential for soil and AD; (ii) medium-priority residues (Boza fermentation residue, mulberry press-cake, fig seed residue, tarhana residues, date syrup filter cake) suited for targeted niches, particularly adsorption and selected energy/environmental uses; and (iii) low-priority residues (saffron floral residue, lupin brining sediment) with low absolute scores even in their best categories. Overall, the SAW-based modelling provides a transparent, decision-oriented basis for aligning Turkey's underutilized food-processing residues with plausible biochar application portfolios, while explicitly acknowledging that rankings can evolve as additional performance or constraint data become available.

Limitations and future work

The SAW-based framework is designed as a transparent, literature-grounded screening tool to prioritise residue–application pathways using the best available physicochemical evidence. Because the dataset is compiled from multiple studies, some methodological variability is expected, and the literature does not report all properties for every residue. To preserve transparency, proxy scores were computed from available indicators with residue-specific weight re-normalisation (Section

"Modelling procedure (SAW–WSM framework)"; Eqs. 4–6), and robustness to plausible weight variation was assessed via sensitivity analysis (Supplementary File 1, Section S1.6). Min–max scaling and linear SAW aggregation enable reproducible comparisons, and the framework is readily extensible as harmonised datasets and application-specific performance measurements (e.g., adsorption tests, key biochar properties, and AD metrics) become available. However, min–max normalisation can be sensitive to extreme values and to small sample sizes, such as the ten-residue dataset considered here. A brief alternative-normalization robustness check using winsorised min–max scaling is provided in Supplementary File 1 (Section S1.6.2), and it indicates that the broad prioritisation pattern remains qualitatively stable, although some within-domain rank shifts occur. Accordingly, the resulting suitability scores should be interpreted as screening-level comparative indicators rather than scale-invariant rankings, and future work should extend this robustness assessment by testing additional normalization schemes, such as z-score or percentile-based scaling, and by examining full-rank stability under broader scenario variation. The present framework should therefore be interpreted as a Phase-1, property-based screening tool rather than a full deployment model. A logical Phase-2 extension would integrate TEA, LCA, logistics, dewatering/drying requirements, seasonal availability, contamination/safety constraints, and end-user acceptance to support deployment-oriented decision-making. Proxy scores derived from incomplete indicator sets should be interpreted with lower confidence than those based on full indicator coverage (Supplementary File 1, Table S3). Accordingly, rankings involving residues or application domains based on lower indicator coverage should be interpreted more cautiously, because omission-based scoring may reduce rank stability relative to cases with more complete proxy support. The SAW framework is fully compensatory, meaning that strong performance in one criterion can offset weakness in another. In practice, however, some variables may function as threshold constraints rather than tradeable attributes, such as high moisture in the absence of drying capacity or ash-related barriers in combustion. Accordingly, the present rankings should be interpreted as screening-level outputs, while future frameworks may incorporate threshold-based or hybrid non-compensatory rules.

Practical implications for stakeholders

The SAW-based suitability indices provide a transparent, literature-grounded screening basis to prioritise residue–application pathways under explicit proxy and weighting assumptions; accordingly, they are intended to support decision-making and targeted validation rather than to serve as stand-alone performance guarantees (Ciardiello and Genovese 2023). High-ranking residues represent near-term candidates for low-cost valorisation, but feasibility is often governed by feedstock handling (e.g., drying/dewatering and size reduction) and transport distance, supporting regionally clustered pre-processing and conversion to reduce logistics burdens and stabilise supply (Anderson et al. 2017).

The prioritisation can inform circular-bioeconomy measures by targeting support to residue-cluster regions, aligning deployment with waste-management requirements, and strengthening biochar quality and end-use safety governance; policy instruments (including subsidies/incentives) are most defensible when linked to measurable quality thresholds and verified outcomes. The screening also identifies where evidence remains proxy-dependent and therefore where pilot-scale trials and application-linked characterisation (e.g., BET/pore structure, surface chemistry, adsorption isotherms/kinetics, soil indicators, and AD performance metrics) are most needed to replace proxies with measured performance data. Because criterion weights reflect the decision logic adopted in this study, the resulting rank order should be interpreted as scenario-dependent rather than universal. Different stakeholder priorities, such as industrial, agricultural, or policy-oriented perspectives, may reasonably produce different rankings.

Conclusion and outlook

This review examined how ten underutilised food-processing residues in Turkey (as a representative agri-food context) can be valorised as biochar feedstocks and how their physicochemical profiles guide thermochemical pathway selection and application alignment. By synthesising reported moisture, ash, fibre-related fractions, HHV and macro-mineral composition, the residues were grouped into practical feedstock classes that map onto plausible conversion routes—hydrothermal carbonisation for high-moisture residues and moderate- to higher-severity slow pyrolysis for drier, energy-dense materials. To translate these property trends into a transparent prioritisation, a SAW-based decision framework was implemented to generate suitability indices across five application domains (fuel, soil amendment, adsorption/remediation, AD enhancement, and composite/material use). Under the adopted criteria and weighting assumptions, rosehip seed cake, pumpkin-seed oil cake and carob syrup pulp residue emerged as consistently high-potential feedstocks, while boza fermentation residue, mulberry press-cake, fig-jam seed fraction, tarhana residues and date syrup filter cake formed an intermediate tier with application-dependent strengths; saffron floral by-product and lupin brining sediment ranked lowest in the current screening. Across domains, adsorption/remediation and fuel exhibited the most consistently high

scores for multiple residues, whereas soil amendment and AD enhancement were more selective, favouring residues with stronger macro-mineral and carbohydrate/protein signatures, respectively.

Beyond the ranking itself, the results provide a preliminary basis for circular bioeconomy planning by indicating where future valorisation pathways may warrant closer assessment. In this context, regionally anchored biochar hubs in Turkey may represent a useful planning direction for future assessment, particularly where residue generation, pre-processing (e.g., dewatering/drying), and conversion capacity could potentially be co-located to reduce transport burdens and improve supply stability. Such configurations may be especially relevant for residue streams that score strongly across multiple outlets (e.g., oilseed- and syrup-processing by-products), while more localised residues may be better suited to smaller-scale or application-specific pathways. At the same time, the decision-support framework is transferable and can be applied beyond Turkey as new region-specific residue datasets become available.

Future research should move from screening to implementation by (i) pilot-scale pyrolysis/HTC trials for the top-ranked residues under application-targeted operating windows; (ii) expanded characterisation using performance-linked metrics (e.g., surface area/pore structure, CEC, pH/alkalinity, adsorption isotherms/kinetics, and AD performance indicators); and (iii) coupling the screening with TEA and LCA to quantify cost and environmental trade-offs under realistic logistics and energy inputs. Finally, integrating residue-to-biochar prioritisation into national and regional waste-management strategies, together with biochar quality and end-use safety standards, may support future scale-up and market uptake. Overall, the proposed framework should be viewed as a first-stage prioritisation tool for transparent residue-to-application screening, rather than as a definitive ranking of real-world biochar suitability.

List of symbols

$i = 1, \ldots, 10$	Index of food-processing residues (boza, tarhana, rosehip seed cake, etc.)
$j = 1, \ldots, M$	Index of physicochemical properties (moisture, ash, HHV, Ca, Mg, K, etc.)
$k = 1, \ldots, K$	Index of mechanistic proxies (fuel quality, nutrient potential, adsorption- oriented screening proxy (Adsorption), AD compatibility, etc.)
$\alpha = 1, \ldots, A$	Index of end-use applications (fuel, soil amendment, adsorption, AD enhancement, composites)
x_{ij}	Raw (measured or compiled) value of property (j) for residue (i)
x_j^{min}, x_j^{max}	Minimum and maximum values of property (j) across all residues
$\tilde{x}_{ij}$	Normalized benefit-type property value for residue (i) and property (j)
$\tilde{x}_{ij}^{(inv)}$	Normalized cost-type (inverted) property value for residue (i) and property (j)
$\hat{x}_{ij}$	Final effective normalized value used in the scoring model
z_{ik}	Mechanistic proxy score for residue (i) under proxy (k)
$w_{\alpha k}$	Base weight assigned to proxy (k) for application (α)
$w'_{\alpha k\|i}$	Re-normalized weight for residue (i) under application (α)
$K_{i\alpha}$	Set of applicable mechanistic proxies for residue (i) in application (α)
$S_{i\alpha}$	Final suitability score for residue (i) in application (α) on a 0–1 scale
$SuitabilityIndex_{i\alpha}$	Suitability index for residue (i) in application (α), scaled to 0–100

Supplementary Information

The online version contains supplementary material available at https://doi.org/10.1186/s40643-026-01067-8.

Supplementary Material 1

Supplementary Material 2

AcknowledgementsPlease add the newly added yellow-highlighted acknowledgement and remove the earlier one.
The authors gratefully acknowledge support from the ECO-SPHERE MSCA COFUND Programme, co-funded by the European Union's Horizon Europe research and innovation programme under the Marie Skłodowska-Curie (Grant Agreement No. 101126655) and Scientific and Technological Research Council of Tüürkiye (TÜÜB˙ITAK) under grant number (123C459).

Author contributions
Ahsanullah Soomro: Conceptualization, Methodology, Investigation, Writing – original draft, Writing – review & editing. Anıl Tevfik Koçer: Visualization, Methodology, Investigation, Formal analysis, Writing – original draft, Writing – review & editing. Didem Balkanlı: Supervision, Writing – review & editing.

FundingPlease add the newly added yellow-highlighted funding and remove the earlier one.
This project has received funding from the European Union's Horizon Europe research and innovation programme under the Marie Skłodowska-Curie grant agreement No. 101126655. This project is also supported in part by a research grant from the Scientific and Technological Research Council of Türkiye (TÜBİTAK) under grant number 123C459.

Data availability
All data supporting the findings of this study are available from the corresponding author upon reasonable request.

Declarations

Ethics approval and consent to participate
Not applicable. This study involved no human participants or animal experiments.

Consent for publication
Not applicable.

Competing interests
The authors declare that they have no competing interests.

Author details
[1]Department of Bioengineering, Yildiz Technical University, 34220 Istanbul, Turkey
[2]Environment Engineering Department, Quaid-e-Awam University of Engineering, Science and Technology (QUEST), Nawabshah, Sindh, Pakistan
[3]Health Biotechnology Joint Research and Application Center of Excellence, 34220 Istanbul, Turkey

Received: 11 December 2025 / Revised: 12 April 2026 / Accepted: 27 April

2026
Published online: 01 June 2026

References

Aboughaly M, Babaei-Ghazvini A, Dhar P, Patel R, Acharya B (2023) Enhancing the potential of polymer composites using biochar as a filler: a review. Polymers 15(19):3981
Agar DA, Hansen P, Rudolfsson M, Blagojević B (2023) Combining behavioural TOPSIS and six multi-criteria weighting methods to rank biomass fuel pellets for energy use in Sweden. Energy Rep 10:706–718
Agegnehu G, Bass AM, Nelson PN, Bird MI (2016) Benefits of biochar, compost and biochar-compost for soil quality, maize yield and greenhouse gas emissions in a tropical agricultural soil. Sci Total Environ 543:295–306
Agegnehu G, Srivastava AK, Bird MI (2017) The role of biochar and biochar-compost in improving soil quality and crop performance: a review. Appl Soil Ecol 119:156–170
Äkräs L, Vahvaselkä M, Silvenius F, Seppälä J, Ilvesniemi H (2022) A multi-criteria decision-making framework and analysis of vegetable oils to produce bio-based plastics. Ind Crops Prod 188:115584
Al-Tarawneh A (2022) Biochar as a cadmium scavenger in the aquatic environment remediation: date seeds as raw material. J Ecol Eng 23(3):270–280
Altıkat A, Alma MH, Altıkat A, Bilgili ME, Altıkat S (2024) A comprehensive study of biochar yield and quality concerning pyrolysis conditions: a multifaceted approach. Sustainability 16(2):937
Anderson NM, Bergman RD, Page-Dumroese DS (2017) A supply chain approach to biochar systems. In: Bruckman V, Varol EA, Uzun B, Liu J (eds) Biochar: a regional supply chain approach in view of climate change mitigation. Cambridge University Press, Cambridge, pp 25–45
Angın D (2013) Effect of pyrolysis temperature and heating rate on biochar obtained from pyrolysis of safflower seed press cake. Bioresour Technol 128:593–597
Ates EB, Gunduz D (2024) Harnessing the energy potential of rosehip wastes towards sustainable energy supply. Process Saf Environ Prot 187:1481–1495
Ayseli MT, Coskun I, Selli S (2023) Evaluation of volatile and thermal properties of boza, a traditional fermented beverage. Microchem J 193:108918
Balagurumurthy B, Srivastava V, Kumar J, Biswas B, Singh R, Gupta P, Kumar KS, Singh R, Bhaskar T (2015) Value addition to rice straw through pyrolysis in hydrogen and nitrogen environments. Bioresour Technol 188:273–279
Banik C, Lawrinenko M, Bakshi S, Laird DA (2018) Impact of pyrolysis temperature and feedstock on surface charge and functional group chemistry of biochars. J Environ Qual 47(3):452–461
Barbeitos CBM (2016) Towards the development of a process for lupin beans detoxification wastewater with lupanine recovery. Master's thesis. Instituto Superior Técnico, Universidade de Lisboa, Lisbon
Baslar M, Ozcelik GN, Calıskan H (2022) A comprehensive review on Beyşehir Tarhana, a Turkish traditional food. Int J Gastron Res 1(1):35–43
Belton V, Stewart T (2012) Multiple criteria decision analysis: an integrated approach. Springer Science & Business Media
Bielecki M, Zubkova V (2023) Analysis of interactions occurring during the pyrolysis of lignocellulosic biomass. Molecules 28(2):506
Bilias F, Kalderis D, Richardson C, Barbayiannis N, Gasparatos D (2023) Biochar application as a soil potassium management strategy: a review. Sci Total Environ 858:159782
Bölek S (2021) Effects of waste fig seed powder on quality as an innovative ingredient in biscuit formulation. J Food Sci 86(1):55–60
Bora NR, Parthiban K, Brahma D, Vishnu MJ, Vasanth V, Rajah RA, Krishnan SN, Bhatt MR, Narzary PR, Dhanush M (2024) Evaluation of mulberry species (*Morus spp.)* as a potential source of bioenergy through thermochemical characterization and gasification. Plant Arch 24(1):1125–1132
Budžaki S, Strelec I, Krnić M, Alilović K, Tišma M, Zelić B (2018) Proximate analysis of cold-press oil cakes after biological treatment with *Trametes versicolor* and *Humicola grisea*. Eng Life Sci 18(12):924–931
Butnaru E, Stoleru E, Ioniță D, Brebu M (2024) Thermal properties of seed cake biomasses and their valorisation by torrefaction. Polymers 16(20):2872
Cárdenas-Aguiar E, Méndez A, Gascó G, Lado M, Paz-González A (2024) The effects of feedstock, pyrolysis temperature, and residence time on the properties and uses of biochar from broom and gorse wastes. Appl Sci 14(10):4283
Chandrasekar R, Prakash P, Ghosh D, Narayanasamy S (2024) Heteroatom doped biochar-aluminosilicate composite as a green alternative for the removal of hazardous dyes: functional characterization and modeling studies. Environ Res 260:119579
Chatterjee R, Sajjadi B, Chen W-Y, Mattern DL, Hammer N, Raman V, Dorris A (2020) Effect of pyrolysis temperature on physicochemical properties and acoustic-based amination of biochar for efficient CO2 adsorption. Front Energy Res 8:85
Ciardiello F, Genovese A (2023) A comparison between TOPSIS and SAW methods. Ann Oper Res 325(2):967–994
Cingöz A, Şahin N (2023) Determination of rheological and chemical properties of hemp, rosehip seed and safflower flours. J Agric Sci 29(4):914–923
Cornelissen G, Nurida NL, Hale SE, Martinsen V, Silvani L, Mulder J (2018) Fading positive effect of biochar on crop yield and soil acidity during five growth seasons in an Indonesian Ultisol. Sci Total Environ 634:561–568
Coşkun F (2014) Tarhananın tarihi ve Türkiye'de tarhana çeşitleri. Gıda Teknol Elektr Derg 9(3):69–79
Criado-Navarro I, Barba-Palomeque F, Pérez-Juan P, Ledesma-Escobar CA, Priego-Capote F (2024) Drying of saffron petals as a critical step for the stabilization of this floral residue prior to extraction of bioactive compounds. Foods 13(23):3724
Crujeira AT, Trancoso MA, Eusébio A, Oliveira AC, Passarinho PC, Abreu M, Marques IP, Marques PA, Marques S, Albergaria H (2023) Admissibility grid to support the decision for the preferential routing of Portuguese endogenous waste biomass for the production of biogas, advanced biofuels, electricity and heat. Biomass 3(4):336–366
Daglioğlu O (2000) Tarhana as a traditional Turkish fermented cereal food. its recipe, production and composition. Food Nahrung 44(2):85–88
Dang D, Mei L, Yan G, Liu W (2023) Synthesis of nanoporous biochar from rice husk for adsorption of methylene blue. J Chem 2023(1):6624295
De Gryze S, Cullen M, Durschinger L, Lehmann J, Bluhm D, Six J, Suddick E (2010) Evaluation of the opportunities for generating carbon offsets from soil sequestration of biochar. In: Climate action reserve, final version, pp 1–99
Demir M, Kahveci Z, Aksoy B, Palapati NK, Subramanian A, Cullinan HT, El-Kaderi HM, Harris CT, Gupta RB (2015) Graphitic biocarbon from metal-catalyzed hydrothermal carbonization of lignin. Ind Eng Chem Res 54(43):10731–10739
Derouich M, Meziani R, Bourkhis B, Filali-Zegzouti Y, Alem C (2020) Nutritional, mineral and organic acid composition of syrups produced from six Moroccan date fruit (*Phoenix dactylifera L.*) varieties. J Food Compos Anal 93:103591
.Do PTM, Nguyen LX (2024) A review of thermochemical decomposition techniques for biochar production. Environ Dev Sustain 1–57.
Dong Z, Li T, Xu X, Chen Y, Fu J, Sun S (2025) Microwave-assisted preparation of hierarchical porous carbon aerogels derived from food wastes for supercapacitors. Nanomaterials 15(5):387
Dursun N (2024) Estimation of pruning wastes and biochar production potential of Turkey. BioResources 19(2):2503–2518
Ege B, Yumrutas O, Ege M, Pehlivan M, Bozgeyik I (2020) Pharmacological properties and therapeutic potential of saffron (*Crocus sativus L.*) in osteosarcoma. J Pharm Pharmacol 72(1):56–67
Erbaş M, Certel M, Uslu MK (2005) Microbiological and chemical properties of Tarhana during fermentation and storage as wet-sensorial properties of Tarhana soup. LWT Food Sci Technol 38(4):409–416
Ermiş S, Yanmaz R (2022) Comparative study of the chemical composition and nutritional value of pumpkin seed (*Cucurbita pepo L.*) grown in the different ecological conditions of Turkey. Türk Tarım Ve Doğa Bilimleri Derg 9(2):413–423
Ertaş N, Bilgiçli N (2014) Effect of different debittering processes on mineral and phytic acid content of lupin (*Lupinus albus L.*) seeds. J Food Sci Technol 51:3348–3354
Esteves T, Mota AT, Barbeitos C, Andrade K, Afonso CA, Ferreira FC (2020) A study on lupin beans process wastewater nanofiltration treatment and lupanine recovery. J Clean Prod 277:123349
Fahim NK, Janati SSF, Feizy J (2012) Chemical composition of agriproduct saffron (*Crocus sativus L.*) petals and its considerations as animal feed. GIDA 37(4):197–201
Feyiz F (2021) Osmanlı şehir mekânlarına bir örnek: Bozahaneler. Uluslararası Ekonomi Siyaset İnsan Ve Toplum Bilimleri Derg 4(1):1–9
Gabhi R, Basile L, Kirk DW, Giorcelli M, Tagliaferro A, Jia CQ (2020) Electrical conductivity of wood biochar monoliths and its dependence on pyrolysis temperature. Biochar 2:369–378
Gai X, Wang H, Liu J, Zhai L, Liu S, Ren T, Liu H (2014) Effects of feedstock and pyrolysis temperature on biochar adsorption of ammonium and nitrate. PLoS ONE 9(12):e113888

Gao N, Du J, Yang W, Li Y, Chen N (2023) Biomass-based shape-stabilized composite phase-change materials with high solar-thermal conversion efficiency for thermal energy storage. Polymers 15(18):3747
García R, Gil M, Fanjul A, González A, Majada J, Rubiera F, Pevida C (2021) Residual pyrolysis biochar as additive to enhance wood pellets quality. Renew Energy 180:850–859
Gaskin JW, Steiner C, Harris K, Das KC, Bibens B (2008) Effect of low-temperature pyrolysis conditions on biochar for agricultural use. Trans ASABE 51(6):2061–2069
Giorcelli M, Bartoli M, Sanginario A, Padovano E, Rosso C, Rovere M, Tagliaferro A (2021) High-temperature annealed biochar as a conductive filler for the production of piezoresistive materials for energy conversion application. ACS Appl Electron Mater 3(2):838–844
Głowacki S, Salamon A, Sojak M, Tulej W, Bryś A, Hutsol T, Salamon M, Kukharets S, Janaszek-Mańkowska M (2022) The use of brewer's spent grain after beer production for energy purposes. Materials 15(10):3703
Gómez AA, Balderas LVN, Moreno CH, Barra JDE (2021) The use of biochar of high growth rate plants to agriculturally remediate heavy metal polluted acidic mine wastes. Recent perspectives in pyrolysis research. IntechOpen
Guo M (2020) The 3R principles for applying biochar to improve soil health. Soil Syst 4(1):9
Halalsheh M, Shatanawi K, Shawabkeh R, Kassab G, Mohammad H, Adawi M, Ababneh S, Abdullah A, Ghantous N, Balah N (2024) Impact of temperature and residence time on sewage sludge pyrolysis for combined carbon sequestration and energy production. Heliyon 10(7):e28685
Harvey OR, Kuo L-J, Zimmerman AR, Louchouarn P, Amonette JE, Herbert BE (2012) An index-based approach to assessing recalcitrance and soil carbon sequestration potential of engineered black carbons (biochars). Environ Sci Technol 46(3):1415–1421
He D, Luo Y, Zhu B (2024) Feedstock and pyrolysis temperature influence biochar properties and its interactions with soil substances: insights from a DFT calculation. Sci Total Environ 922:171259
Hoekstra E, van Swaaij WP, Kersten SR, Hogendoorn KJ (2012) Fast pyrolysis in a novel wire-mesh reactor: design and initial results. Chem Eng J 191:45–58
Hosseini A, Razavi BM, Hosseinzadeh H (2018) Saffron (*Crocus sativus*) petal as a new pharmacological target: a review. Iran J Basic Med Sci 21(11):1091
Hosseinzaei B, Hadianfard MJ, Ruiz-Rosas R, Rosas JM, Rodríguez-Mirasol J, Cordero T (2022) Effect of heating rate and H_3PO_4 as catalyst on the pyrolysis of agricultural residues. J Anal Appl Pyrolysis 168:105724
Huang S, Wu Q, Zhou D, Huang R (2015) Thermal decomposition properties of materials from different parts of corn stalk. BioResources 10(2):2020–2031
Huff MD, Lee JW (2016) Biochar-surface oxygenation with hydrogen peroxide. J Environ Manag 165:17–21
Inyang M, Gao B, Yao Y, Xue Y, Zimmerman AR, Pullammanappallil P, Cao X (2012) Removal of heavy metals from aqueous solution by biochars derived from anaerobically digested biomass. Bioresour Technol 110:50–56
Iticha B, Mosley LM, Marschner P (2024) Combining lime and organic amendments based on titratable alkalinity for efficient amelioration of acidic soils. Soil 10(1):33–47
Karakaş C, Özçimen D, İnan B (2017) Potential use of olive stone biochar as a hydroponic growing medium. J Anal Appl Pyrolysis 125:17–23
Katnić Đ, Marinović-Cincović M, Porobić SJ, Vujčić I, Šaponjić A, Sikirić B, Živojinović D (2022) Characterization and kinetics of thermal decomposition behavior of plum and fig pomace biomass. J Clean Prod 352:131637
Kattil A, Dash KK, Shams R, Sharma S (2024) Nutritional composition, phytochemical extraction, and pharmacological potential of mulberry: a comprehensive review. Future Foods 9:100295
Kaushik A, Priyadharshini P, Palaniselvam V, Parthiban K, Manimegalai S (2025) Characterization of mulberry biochar: implications for sustainable agriculture. J Biobased Mater Bioenergy 19(1):58–65
Khalid L, Jabeen I, Ahmad T, Inam-ur-Raheem M, Shahid A, Cirillo T, Esposito F (2025) Valorization of fruit and vegetable by-products for protein extraction and their functional applications in food and non-food sectors. Food Bioprod Process 154:198–215
Kim J-S, Park K-B (2020) Production of phenols by lignocellulosic biomass pyrolysis. In: Fang Z, Smith RL, Xu L (eds) Production of biofuels and chemicals with pyrolysis. Springer, Singapore, pp 289–319
Kıvanç M, Funda EG (2017) A functional food: a traditional Tarhana fermentation. Food Sci Technol 37(2):269–274
Kizil S, Toncer O, Sogut T (2018) Mineral contents and fatty acid compositions of wild and cultivated rose hip (*Rosa canina L.*). Fresenius Environ Bull 27(2):744–748
Koçer AT, İnan B, KaptanUsul S, Özçimen D, Yılmaz MT, Işıldak İ (2021) Exopolysaccharides from microalgae: production, characterization, optimization and techno-economic assessment. Braz J Microbiol 52(4):1779–1790
Koçer AT, İnan B, Özçimen D (2018) A comparison of bioethanol and biochar production from various algal biomass samples and sweet sorghum energy crop. Environ Res Technol 1(1):43–50
Koçer AT, Karacaoğlu B, Karaca GA, İnan B, Balkanlı D (2024) Thermal behavior analysis and biochar formation through co-pyrolysis of de-oiled microalgae biomass and wood sawdust for ecofriendly resource utilization. Algal Res 82:103674
Koçer AT, Mutlu B, Özçimen D (2020) Investigation of biochar production potential and pyrolysis kinetics characteristics of microalgal biomass. Biomass Convers Bioref 10(1):85–94
Koçer AT, Özçimen D (2018) Investigation of the biogas production potential from algal wastes. Waste Manag Res 36(11):1100–1105
Koçer AT, Özçimen D (2024) Determination of combustion characteristics and kinetic parameters of *Ulva lactuca* and its biochar. Biomass Convers Bioref 14(5):5913–5922
Kopp Alves A, Hauschild T, Basegio TM, Amorim Berutti F (2024) Influence of lignin and cellulose from termite-processed biomass on biochar production and evaluation of chromium VI adsorption. Sci Rep 14(1):14937
Kosakowski W, Bryszewska MA, Dziugan P (2020) Biochars from post-production biomass and waste from wood management: analysis of carbonization products. Materials 13(21):4971
Köse E, Yücel U (2003) Chemical composition of boza. J Food Technol 1(4):191–193
Kültür Ş, Eraslan ZB (2023) The genus *Rosa* L. In: Koçyiğit M, Arıcan YE, Haspolat YK (eds) Rosa. Orient Publications, Ankara, pp 26–41
Kwapinska M, Pisano I, Leahy JJ (2023) Hydrothermal carbonization of milk/dairy processing sludge: fate of plant nutrients. J Environ Manag 345:118931
Lago BC, Silva CA, Melo LCA, de Morais EG (2021) Predicting biochar cation exchange capacity using Fourier transform infrared spectroscopy combined with partial least square regression. Sci Total Environ 794:148762
Lefebvre D, Fawzy S, Aquije CA, Osman AI, Draper KT, Trabold TA (2023) Biomass residue to carbon dioxide removal: quantifying the global impact of biochar. Biochar 5(1):65
Li Y, Meng Q, Zhou B, Zhou Z (2017) Effect of ensiled mulberry leaves and sun-dried mulberry fruit pomace on the fecal bacterial community composition in finishing steers. BMC Microbiol 17(1):97
Lima DR, Lima EC, Thue PS, Dias SL, Machado FM, Seliem MK, Sher F, dos Reis GS, Saeb MR, Rinklebe J (2021) Comparison of acidic leaching using a conventional and ultrasound-assisted method for preparation of magnetic-activated biochar. J Environ Chem Eng 9(5):105865
Limwikran T, Kheoruenromne I, Suddhiprakarn A, Prakongkep N, Gilkes R (2018) Dissolution of K, Ca, and P from biochar grains in tropical soils. Geoderma 312:139–150
Liu C, Ye J, Lin Y, Wu X, Price G, Wang Y (2024) Effect of natural aging on biochar physicochemical property and mobility of Cd (II). Sci Rep 14(1):22214
Liu L, Yuan M, Wang X, Li X, Fang W, Shan D, Dai Y (2021) Biochar aging: properties, mechanisms, and environmental benefits for adsorption of metolachlor in soil. Environ Technol Innov 24:101841
Liu W-J, Jiang H, Yu H-Q (2015) Development of biochar-based functional materials: toward a sustainable platform carbon material. Chem Rev 115(22):12251–12285
Liu Z, Niu W, Chu H, Zhou T, Niu Z (2018) Effect of the carbonization temperature on the properties of biochar produced from the pyrolysis of crop residues. BioResources 13(2):3429–3446
Lu X, Gu X (2022) A review on lignin pyrolysis: pyrolytic behavior, mechanism, and relevant upgrading for improving process efficiency. Biotechnol Biofuels Bioprod 15(1):106
Lua AC, Guo J (2000) Activated carbon prepared from oil palm stone by one-step CO2 activation for gaseous pollutant removal. Carbon 38(7):1089–1097
Luan J, Wang Q, Shao D, Cui B, Han P, He Q (2025) Research progress on influencing factors and control methods of slagging in biomass combustion. Front Energy Res 13:1634354
Mahmood F, Ali M, Khan M, Mbeugang CFM, Isa YM, Kozlov A, Penzik M, Xie X, Yang H, Zhang S (2025) A review of biochar production and its employment in synthesizing carbon-based materials for supercapacitors. Ind Crops Prod 227:120830
Maniscalco M, Infurna G, Caputo G, Botta L, Dintcheva NT (2021) Slow pyrolysis as a method for biochar production from carob waste: process investigation and products' characterization. Energies 14(24):8457

Marrot L, Candelier K, Valette J, Lanvin C, Horvat B, Legan L, DeVallance DB (2022) Valorization of hemp stalk waste through thermochemical conversion for energy and electrical applications. Waste Biomass Valor 13(4):2267–2285
Mihajlović I, Hgeig A, Novaković M, Gvoić V, Ubavin D, Petrović M, Kurniawan TA (2025) Valorizing date seeds into biochar for pesticide removal: a sustainable approach to agro-waste-based wastewater treatment. Sustainability 17(11):5129
Milala J, Kosmala M, Sójka M, Kołodziejczyk K, Klewicki R, Król M, Karlińska E, Rój E (2023) *Rosa rugosa* low caloric fiber protein preparations rich in antioxidant flavanols and ellagitannins. Molecules 28(24):8021
Mishra R, Gollakota AR, Shu C-M (2024) Cultivating eco-advantages: unleashing the distinctive potential of biochar in microbial fuel cells. Process Saf Environ Prot 185:614–631
Mohan D, Sarswat A, Ok YS, Pittman CU Jr (2014) Organic and inorganic contaminants removal from water with biochar, a renewable, low cost and sustainable adsorbent-a critical review. Bioresour Technol 160:191–202
Molina-Sabio M, Rodríguez-Reinoso F (2004) Role of chemical activation in the development of carbon porosity. Colloids Surf A Physicochem Eng Asp 241(1–3):15–25
Morgan TJ, Turn SQ, George A (2015) Fast pyrolysis behavior of banagrass as a function of temperature and volatiles residence time in a fluidized bed reactor. PLoS ONE 10(8):e0136511
Morgano MT, Bergfeldt B, Leibold H, Richter F, Stapf D (2018) Intermediate pyrolysis of agricultural waste: a decentral approach towards circular economy. Chem Eng Trans 65:261–266
Musa Özcan M, Arslan D, Gökçalik H (2007) Some compositional properties and mineral contents of carob (*Ceratonia siliqua*) fruit, flour and syrup. Int J Food Sci Nutr 58(8):652–658
Naeem MA, Khalid M, Arshad M, Ahmad R (2014) Yield and nutrient composition of biochar produced from different feedstocks at varying pyrolytic temperatures. Pak J Agric Sci 51(1):75–82
Nakilcioğlu-Taş E (2019) Biochemical characterization of fig (*Ficus carica L.*) seeds. J Agric Sci 25(2):232–237
Nan H, Jiang Y, Zhou W, Zhao L, Yang F (2023) New insights into the enhancement effect of exogenous calcium on biochar stability during its aging in farmland soil. Agronomy 13(7):1676
Ndibize WE, Hossain MN, Hongyan N, Salam M, Mian MM, Sarker ME, Shojib MRI (2022) Ammonium-nitrogen removal from aqueous solution using municipal green waste wood biochars. Adv Environ Technol 8(1):15–29
Ngene GI, Bouesso B, Martínez MG, Nzihou A (2024) A review on biochar briquetting: common practices and recommendations to enhance mechanical properties and environmental performances. J Clean Prod 469:143193
Ngo T, Khudur LS, Hassan S, Jansriphibul K, Ball AS (2024) Enhancing microbial viability with biochar for increased methane production during the anaerobic digestion of chicken manure. Fuel 368:131603
Nguyen AT, Bui TA, Mai NT, Tran HT, Tran SV, Nguyen NH, Tsubota T, Shinogi Y, Dultz S, Nguyen MN (2020) Release kinetics of potassium from silica-rich fern-derived biochars. Agron J 112(3):1713–1725
Novák A, Kovács B, Czipa N (2016) Variation of boza nutrition parameters based on raw materials. Acta Agrar Debr 67:67–70
Nunes LJ (2020) Torrefied biomass as an alternative in coal-fueled power plants: a case study on grindability of agroforestry waste forms. Clean Technol Environ Policy 2(3):270–289
Nunes LJ, Rodrigues AM, Matias JC, Ferraz AI, Rodrigues AC (2021) Production of biochar from vine pruning: waste recovery in the wine industry. Agriculture Basel 11(6):489
Oladzad S, Fallah N, Mahboubi A, Afsham N, Taherzadeh MJ, Toghyani J (2024) Comparison of acid and hydrothermal pretreatments of date waste for value creation. Sci Rep 14:18056
Omara P, Singh H, Singh K, Sharma L, Otim F, Obia A (2023) Short-term effect of field application of biochar on cation exchange capacity, pH, and electrical conductivity of sandy and clay loam temperate soils. Technol Agron 3:16
Ozbay G, Ayrilmis N (2017) Effect of pyrolysis temperature on bio-oil production from vacuum pyrolysis of waste from wood industry. In: Proceedings of the 117th IIER international conference, Helsinki, Finland, 17–18 Aug 2017, pp 56–58
Özçimen D (2013) An approach to the characterization of biochar and bio-oil. In: Lohani SP (ed) Renewable energy for sustainable future. iConcept Press, Kowloon, pp 41–58
Özçimen D, Ersoy-Meriçboyu A (2008) A study on the carbonization of grapeseed and chestnut shell. Fuel Process Technol 89(11):1041–1046
Özçimen D, İnan B, Akış S, Koçer AT (2015) Utilization alternatives of algal wastes for solid algal products. In: Jacob-Lopes E, Queiroz Zepka L, Queiroz MI (eds) Algal biorefineries: volume 2: products and refinery design. Springer, Cham, pp 393–418
Özçimen D, İnan B, Koçer AT, Vehapi M (2018) Bioeconomic assessment of microalgal production. In: Jacob-Lopes E, Zepka LQ, Queiroz MI (eds) Microalgal biotechnology. IntechOpen, London, pp 195–213
Ozrenk K, Gazioglu S, Erdinc C, Guleryuz M, Aykanat A (2010) Molecular characterization of mulberry germplasm from Eastern Anatolia. Afr J Biotechnol 9(1):001–006
Özyurtkan MH, Özçimen D, Meriçboyu AE (2008) Investigation of the carbonization behavior of hybrid poplar. Fuel Process Technol 89(9):858–863
Pahnila M, Koskela A, Sulasalmi P, Fabritius T (2023) A review of pyrolysis technologies and the effect of process parameters on biocarbon properties. Energies 16(19):6936
Paritosh K, Kushwaha SK, Yadav M, Pareek N, Chawade A, Vivekanand V (2017) Food waste to energy: an overview of sustainable approaches for food waste management and nutrient recycling. Biomed Res Int 2017(1):2370927
Parmaki S (2022) A novel microbial approach for the valorisation of lupanine containing wastewater emitted from the lupin beans processing industry. PhD thesis, Cyprus University of Technology, Limassol.
Paula R, Carvalho J, Júnior A, Fagundes F, de Lima R, Lima E, Oliveira C, de Oliveira M, Bezerra A, Ferreira O (2025) Analysis of biochar-cement composites by SEM/EDS: interfacial interactions and effects on mechanical strength. C 11(3):45
Paulette T (2024) In the land of Ninkasi: a history of beer in ancient Mesopotamia. Oxford University Press, New York
Petrovič A, Predikaka TC, Vohl S, Hostnik G, Finšgar M, Čuček L (2024) Hydrothermal conversion of oilseed cakes into valuable products: influence of operating conditions and whey as an alternative process liquid on product properties and their utilization. Energy Convers Manag 313:118640
Pierrehumbert RT (2014) Short-lived climate pollution. Annu Rev Earth Planet Sci 42(1):341–379
Piga A, Ponce CV, Aksoy U (2022) Fig products from tradition to future. Advances in fig research and sustainable production. CABI, Wallingford, pp 441–455
Qian C, Li Q, Zhang Z, Wang X, Hu J, Cao W (2020) Prediction of higher heating values of biochar from proximate and ultimate analysis. Fuel 265:116925
Raza M, Inayat A, Ahmed A, Jamil F, Ghenai C, Naqvi SR, Shanableh A, Ayoub M, Waris A, Park Y-K (2021) Progress of the pyrolyzer reactors and advanced technologies for biomass pyrolysis processing. Sustainability 13(19):11061
Reis Portilho G, Resende de Castro V, de Cássia Oliveira Carneiro A, Cola Zanuncio J, José VinhaZanuncio A, Gabriella Surdi P, Gominho J, de Oliveira Araújo S (2020) Potential of briquette produced with torrefied agroforestry biomass to generate energy. Forests 11(12):1272
Román S, Ledesma B, Álvarez-Murillo A, Al-Kassir A, Yusaf T (2017) Dependence of the microporosity of activated carbons on the lignocellulosic composition of the precursors. Energies 10(4):542
Romão EL, Conte RA (2021) Energy gains of Eucalyptus by torrefaction process. Maderas Cienc Tecnol 23(3):1–6
Şahin G, Taşlıgil N (2016) Agricultural geography analysis of carob tree (*Ceratonia siliqua* L.) from Turkey. Turk J Agric 4(12):1192–1200
Sajjadi B, Chen W-Y, Egiebor NO (2019) A comprehensive review on physical activation of biochar for energy and environmental applications. Rev Chem Eng 35(6):735–776
Saletnik B, Inglot D, Findura P, Puchalski C, Bd J (2025) Pyrolysis valorisation of fruit processing residues: energy and emission potential of apricot (*Prunus armeniaca L.*) and cornelian cherry (*Cornus mas L.)* seed biochar. Int Agrophys 40(1):55–66
Şekkeli Z, Kaya E, Erdem TK, Tekin FB (2015) A research on determination of supply types of Maras tarhana at Kahramanmaras Vocational School students. Int J Sci Technol Res 1(2):31–41
Sharma B, Vaish B, Monika SUK, Singh P, Singh RP (2019) Recycling of organic wastes in agriculture: an environmental perspective. Int J Environ Res 13(2):409–429
Sharma T, Hakeem IG, Gupta AB, Joshi J, Shah K, Vuppaladadiyam AK, Sharma A (2024) Parametric influence of process conditions on thermochemical techniques for biochar production: a state-of-the-art review. J Energy Inst 113:101559
Sheir MA (2022) Innovative use of date (*Phoenix dactylifera L.*) press cake in the food industry. Foods Raw Mater 10(1):2–9
Shen Y, Zhao P, Shao Q, Takahashi F, Yoshikawa K (2015) In situ catalytic conversion of tar using rice husk char/ash supported nickel-iron catalysts for biomass

pyrolytic gasification combined with the mixing-simulation in fluidized-bed gasifier. Appl Energy 160:808–819
Shim JH, Patel R (2024) Progress in nanofiltration-based capacitive deionization. Membr J 34(2):87–95
Siddiqua A, Hahladakis JN, Al-Attiya WAK (2022) An overview of the environmental pollution and health effects associated with waste landfilling and open dumping. Environ Sci Pollut Res 29(39):58514–58536
Sieradzka M, Jerzak W, Mlonka-Mędrala A, Marszałek A, Dudziak M, Kalemba-Rec I, Błoniarz A, Reinmöller M, Kopia A, Nowak W (2025) Valorisation of food industry waste into high-performance biochar for environmental applications. Sci Rep 15(1):26195
Singh A, Tirpude A, Mathew N, Arfin T (2025) Gaseous emissions from solid waste disposal. Waste derived carbon nanomaterials, vol 1. ACS Publications, pp 95–114
Singh H, Northup BK, Rice CW, Prasad PV (2022) Biochar applications influence soil physical and chemical properties, microbial diversity, and crop productivity: a meta-analysis. Biochar 4(1):8
Singh J (2006) The role of inhibitors in mitigating nitrogen losses from cattle urine and nitrogen fertiliser inputs in pastures: a thesis presented in partial fulfilment of the requirements for the degree of Doctor of Philosophy (Ph.D.) in Soil Science at Massey University, Palmerston North, New Zealand. PhD thesis. Massey University, Palmerston North.
Sinkovic L, Kolmanic A (2021) Elemental composition and nutritional characteristics of *Cucurbita pepo subsp. pepo* seeds, oil cake and pumpkin oil. J Elem 26(1):97–107
Sivaranjanee R, Kumar PS, Chitra B, Rangasamy G (2024) A critical review on biochar for the removal of toxic pollutants from water environment. Chemosphere 360:142382
Skrzypczak D, Mironiuk M, Witek-Krowiak A, Mikula K, Pstrowska K, Łużny R, Mościcki K, Pawlak-Kruczek H, Siarkowska A, Moustakas K (2024) Innovative fertilizers and soil amendments based on hydrochar from brewery waste. Clean Technol Environ Policy 26(5):1571–1586
Spokas KA (2010) Review of the stability of biochar in soils: predictability of O:C molar ratios. Carbon Manag 1(2):289–303
Sun J, He F, Pan Y, Zhang Z (2017) Effects of pyrolysis temperature and residence time on physicochemical properties of different biochar types. Acta Agric Scand B Soil Plant Sci 67(1):12–22
Ta TMN, Hoang CH, Nguyen TM, Tran TTT, Ton NMN, Le VVM (2023) Effects of mulberry pomace addition and transglutaminase treatment on the quality of pasta enriched with antioxidants and dietary fiber. Pol J Food Nutr Sci 73(4):301–310
Taherdoost H (2023) Analysis of simple additive weighting method (SAW) as a multi-attribute decision-making technique: a step-by-step guide. J Manag Sci Eng Res 6(1):21–24
Talwar P, Agudelo MA, Nanda S (2025) Pyrolysis process, reactors, products, and applications: a review. Energies 18(11):2979
Tamer CE, Kumral A, Aşan M, Şahin İ (2007) Chemical compositions of traditional tarhana having different formulations. J Food Process Preserv 31(1):116–126
Tan X-F, Zhu S-S, Wang R-P, Chen Y-D, Show P-L, Zhang F-F, Ho S-H (2021) Role of biochar surface characteristics in the adsorption of aromatic compounds: pore structure and functional groups. Chin Chem Lett 32(10):2939–2946
Tang L, Huang H (2005) Plasma pyrolysis of biomass for production of syngas and carbon adsorbent. Energy Fuels 19(3):1174–1178
Taylor MJ, Alabdrabalameer HA, Michopoulos AK, Volpe R, Skoulou V (2020) Augmented leaching pretreatments for forest wood waste and their effect on ash composition and the lignocellulosic network. ACS Sustain Chem Eng 8(14):5674–5682
Thi DP, Hang NNT, Viet OT, Van LN, Viet AN, Lan PDT, Van NV (2021) Sandy soil reclamation using biochar and clay-rich soil. J Ecol Eng 22(6):26–35
Tomczyk A, Sokołowska Z, Boguta P (2020) Biochar physicochemical properties: pyrolysis temperature and feedstock kind effects. Rev Environ Sci Biotechnol 19(1):191–215
Tounsi L, Karra S, Kechaou H, Kechaou N (2017) Processing, physico-chemical and functional properties of carob molasses and powders. J Food Meas Charact 11:1440–1448
Triantaphyllou E (2000) Multi-criteria decision making methods: a comparative study. Springer, New York
Tzeng G-H, Huang J-J (2011) Multiple attribute decision making: methods and applications. CRC Press, Boca Raton
Vafaei N, Ribeiro RA, Camarinha-Matos LM (2016) Normalization techniques for multi-criteria decision making: analytical hierarchy process case study. In: Camarinha-Matos LM, Falcão AJ, Vafaei N, Najdi S (eds) Technological innovation for cyber-physical systems. DoCEIS 2016. IFIP Adv Inf Commun Technol, vol 470. Springer, Cham, pp 261–269.
Vafaei N, Ribeiro RA, Camarinha-Matos LM (2022) Assessing normalization techniques for simple additive weighting method. Procedia Comput Sci 199:1229–1236
Valentin MT, Luo G, Zhang S, Białowiec A (2023) Direct interspecies electron transfer mechanisms of a biochar-amended anaerobic digestion: a review. Biotechnol Biofuels Bioprod 16(1):146
Vehapi M, Yılmaz A, Özçimen D (2018) Antifungal activities of *Chlorella vulgaris* and *Chlorella minutissima* microalgae cultivated in Bold Basal medium, wastewater and tree extract water against *Aspergillus niger* and *Fusarium oxysporum*. Rom Biotechnol Lett 1:1–8
Wallace CA, Afzal MT, Saha GC (2019) Effect of feedstock and microwave pyrolysis temperature on physio-chemical and nano-scale mechanical properties of biochar. Bioresour Bioprocess 6(1):1–11
Wang B, Lehmann J, Hanley K, Hestrin R, Enders A (2016) Ammonium retention by oxidized biochars produced at different pyrolysis temperatures and residence times. RSC Adv 5(98):80613–80622
Wang G, Dai Y, Yang H, Xiong Q, Wang K, Zhou J, Li Y, Wang S (2020) A review of recent advances in biomass pyrolysis. Energy Fuels 34(12):15557–15578
Wang W, Li X, Zhang W, Wang Y (2023) Porous carbon materials derived from biomass waste as efficient electrodes for capacitive deionization desalination. Desalin Water Treat 306:131–150
Wang Y, Yu S, Yuan H, Zhang L (2024) Constructing N, S co-doped network biochar confined $CoFe_2O_4$ magnetic nanoparticles adsorbent: insights into the synergistic and competitive adsorption of Pb2+ and ciprofloxacin. Environ Pollut 343:123178
Weng ZH, Cowie AL (2025) Estimates vary but credible evidence points to gigaton-scale climate change mitigation potential of biochar. Commun Earth Environ 6(1):259
Wystalska K, Kwarciak-Kozłowska A (2021) The effect of biodegradable waste pyrolysis temperatures on selected biochar properties. Materials 14(7):1644
Xia S, Yang H, Lu W, Cai N, Xiao H, Chen X, Chen Y, Wang X, Wang S, Wu P (2022) Fe-Co based synergistic catalytic graphitization of biomass: influence of the catalyst type and the pyrolytic temperature. Energy 239:122262
Xiao X, Chen Z, Chen B (2016) H/C atomic ratio as a smart linkage between pyrolytic temperatures, aromatic clusters and sorption properties of biochars derived from diverse precursory materials. Sci Rep 6(1):22644
Xu X, Wu Y, Wu X, Sun Y, Huang Z, Li H, Wu Z, Zhang X, Qin X, Zhang Y (2022) Effect of physicochemical properties of biochar from different feedstock on remediation of heavy metal contaminated soil in mining area. Surf Interfaces 32:102058
Yan Q, Toghiani H, Yu F, Cai Z, Zhang J (2011) Effects of pyrolysis conditions on yield of bio-chars from pine chips. For Prod J 61(5):367–371
Yang H, Yan R, Chen H, Lee DH, Zheng C (2007) Characteristics of hemicellulose, cellulose and lignin pyrolysis. Fuel 86(12–13):1781–1788
Yang Q, Liu H, Liu L, Yan Z, Chui C, Yang N, Wang C, Shen G, Chen Q (2025) Enhancing methane production in anaerobic digestion of food waste using co-pyrolysis biochar derived from digestate and rice straw. Molecules 30(8):1766
Yao Y, Yao T, Qian C (2025) Synthesis and application for Pb^{2+} removal of a novel magnetic biochar embedded with FexOy nanoparticles. Symmetry 17(4):516
Yegin S, Fernández-Lahore M (2012) Boza, a traditional cereal-based, fermented Turkish beverage. In: Hui YH (ed) Handbook of plant-based fermented food and beverage technology, 2nd edn. CRC Press, Boca Raton, pp 341–357
Yildiz G, Ronsse F, Venderbosch R, van Duren R, Kersten SR, Prins W (2015) Effect of biomass ash in catalytic fast pyrolysis of pine wood. Appl Catal B Environ 168:203–211
Yousif AK, Alghzawi H (2000) Processing and characterization of carob powder. Food Chem 69(3):283–287
Yuan JH, Xu RK (2011) The amelioration effects of low temperature biochar generated from nine crop residues on an acidic Ultisol. Soil Use Manag 27(1):110–115

Publisher's note

Springer Nature remains neutral with regard to jurisdictional claims in published maps and institutional affiliations.